NACA

RESEARCH MEMORANDUM

AN INVESTIGATION AT TRANSONIC SPEEDS OF THE EFFECTS OF THICKNESS RATIO AND OF THICKENED ROOT SECTIONS ON THE AERODYNAMIC CHARACTERISTICS OF WINGS WITH 47° SWEEPBACK, ASPECT RATIO 3.5, AND TAPER RATIO 0.2 IN THE SLOTTED TEST SECTION OF THE LANGLEY 8-FOOT HIGH-SPEED TUNNEL

By Ralph P. Bielat, Daniel E. Harrison,
and Domenic A. Coppolino

Langley Aeronautical Laboratory
Langley Field, Va.

NATIONAL ADVISORY COMMITTEE
FOR AERONAUTICS

WASHINGTON

October 31, 1951

Classification cancelled (or changed to UNCLASSIFIED)

By authority of NASA Tech Pub Announcement #4

(OFFICER AUTHORIZED TO CHANGE)

By M Boss

NAME AND

GMB

GRADE OF OFFICER MAKING CHANGE)

20 Mar 61

DATE

NATIONAL ADVISORY COMMITTEE FOR AERONAUTICS

RESEARCH MEMORANDUM

AN INVESTIGATION AT TRANSONIC SPEEDS OF THE EFFECTS OF THICKNESS RATIO AND OF THICKENED ROOT SECTIONS ON THE AERODYNAMIC CHARACTERISTICS OF WINGS WITH 47° SWEEPBACK, ASPECT RATIO 3.5, AND TAPER RATIO 0.2 IN THE SLOTTED TEST SECTION OF THE LANGLEY 8-FOOT HIGH-SPEED TUNNEL

By Ralph P. Bielat, Daniel E. Harrison, and Domenic A. Coppolino

SUMMARY

Four wing-body combinations of the same plan form (47° sweep, 3.5 aspect ratio, and 0.2 taper ratio) were compared at transonic speeds in the Langley 8-foot high-speed tunnel. Three wings were 4, 6, and 9 percent thick; the fourth was 6 percent thick but, on the inner 0.4 span, tapered to 12-percent thickness at the roots.

In general, reducing wing thickness ratio improved the transonic characteristics. Near zero lift, the thinnest wing nearly doubled its lift-curve slope at the high subsonic Mach numbers; the others increased somewhat less. Similar but less pronounced effects were found at a lift coefficient of 0.3. At a Mach number of 1.10, the zero-lift drag coefficients for the 4-, 6-, and 9-percent-thick wings were higher than the low-speed values by factors of approximately 2, 2.4, and 4, respectively.

A comparison of the values of maximum lift-drag ratios $(L/D)_{max}$ at a Mach number of 0.925 indicated that reducing the wing thickness ratios resulted in an increase in the $(L/D)_{max}$ values from 15.0 for the 9-percent-thick wing to 18.3 for the 6-percent-thick wing, and to 25.0 for the 4-percent-thick wing. At a Mach number of 1.10, decreasing the wing thickness ratio from 9 to 4 percent increased the $(L/D)_{max}$ value by a factor of 1.7.

As the Mach number increased from 0.50 to 1.10, the aerodynamic center for the 9-percent-thick wing moved rearward 11 percent as compared with a 15-percent rearward movement for the 4- and 6-percent-thick wings.

The characteristics of the 6-percent-thick wing with the thickened inboard sections were approximately intermediate between those of the 6- and 9-percent-thick wings.

INTRODUCTION

Four wing-body combinations of the same plan form (47° sweep, 3.5 aspect ratio, and 0.2 taper ratio) were compared at transonic speeds in the Langley 8-foot high-speed tunnel. Three wings were 4, 6, and 9 percent thick; the fourth was 6 percent thick but, on the inner 0.4 span, tapered to 12-percent thickness at the roots.

The results reported herein consisted of lift, drag, and pitching-moment measurements for a Mach number range of 0.50 to approximately 1.12. Only a limited analysis of the data has been included in this paper in order to expedite publication of the data.

SYMBOLS

C_D	drag coefficient (D/qS)
$\frac{dC_D}{dC_L^2}$	drag-due-to-lift parameter
C_{D_o}	drag coefficient at zero lift
C_L	lift coefficient (L/qS)
C_{L_α}	lift-curve slope per degree $\left(dC_L/d\alpha\right)$
C_m	pitching-moment coefficient $\left(\frac{M_{\bar{c}/4}}{qS\bar{c}}\right)$
$\frac{dC_m}{dC_L}$	static-longitudinal-stability parameter
$\bar{c}$	wing mean aerodynamic chord, inches

D	drag, pounds
L	lift, pounds
$(L/D)_{max}$	maximum lift-drag ratio
M	Mach number
$M_{\bar{c}/4}$	pitching moment about $0.25\bar{c}$, inch-pounds
q	free-stream dynamic pressure, pounds per square foot $\left(\frac{1}{2}\rho V^2\right)$
R	Reynolds number based on $\bar{c}$
S	wing area, square feet
t/c	wing thickness ratio in percent of chord
V	free-stream velocity, feet per second
α	angle of attack of body center line, degrees
ρ	free-stream density, slugs per cubic foot

APPARATUS AND METHODS

Tunnel

The tests were conducted in the slotted test section of the Langley 8-foot high-speed tunnel. The use of longitudinal slots in the test section permitted the testing of the models through the speed of sound without the usual choking effects found in the conventional closed-throat type of wind tunnel. Typical Mach number distributions along the center of the slotted test section in the region occupied by the model are shown in figure 1. A complete description of the slotted test section of the Langley 8-foot high-speed tunnel can be found in reference 1.

Model

The models employed for the tests were supplied by a U. S. Air Force contractor. The models represented midwing configurations and were constructed of steel. All the models had the same wing plan form, with 47° sweepback of the 0.25-chord line, aspect ratio of 3.5, taper ratio

of 0.2, zero twist and dihedral, and the following airfoil section parallel to the model plane of symmetry:

Thickness distribution . . . . . NACA 65A-series

Mean line ordinates . . . 1/3 of NACA 230 series + NACA 6-series uniform-load mean line (a = 1.0) for $C_{l_i} = 0.1$

The only differences in the models were the wing thickness ratios and the spanwise thickness distribution. The hollow steel bodies were built integrally with each of the wings and represented cylindrical bodies having ogive nose sections. A photograph of wing model 1 is shown in figure 2 and dimensional details of the models are shown in figure 3. Airfoil coordinates for the various models are given in table I.

Model Support System

The models were attached to the sting support through a six-component, internal, electrical strain-gage balance which was provided by a U. S. Air Force contractor. Angle-of-attack changes of the models were accomplished by pivoting the sting about a point which was located approximately 66 inches downstream of the 0.25 mean aerodynamic chord. A 15° coupling located ahead of the pivot point was used in order to keep the model position reasonably close to the tunnel axis when the model angle of attack was varied from 6° to 12°. The angle mechanism was controlled from outside the test section and therefore permitted angle changes with the tunnel operating. A detailed description of the support system can be found in reference 2.

Measurements

Lift, drag, and pitching moment were determined by means of an electrical strain-gage balance located inside the body. The measurements were made for angles of attack from -2° to 12° at Mach numbers varying from 0.50 to approximately 0.97 and from -2° to 4° at Mach numbers varying from 1.00 to approximately 1.12. Testing at higher angles of attack in the supersonic range was ruled out by the pitching-moment design load of the balance. The accuracy of the data, based on the design of the balance and the reproducibility of the data, is as follows:

C_L . . . . . ±0.01

C_D . . . . . ±0.001

C_m . . . . . ±0.004

A pendulum-type accelerometer calibrated against angle of attack located within the sting downstream of the models was used to indicate the angles of the models relative to the air stream. It was necessary to apply a correction to the angle of attack of the model because of the elasticity of the sting-support system. The corrections were obtained from static calibrations of the sting and the results are shown in figure 4.

The use of the calibrated accelerometer in conjunction with the remotely controlled angle-of-attack changing mechanism allowed the model angle to be set within $\pm 0.1^\circ$ for all test Mach numbers.

Reynolds Number

The variation of test Reynolds number, based on the mean aerodynamic chord of the wing, with Mach number averaged for several runs is presented in figure 5. The Reynolds number varied from 2.0×10^6 at a Mach number of 0.50 to 2.5×10^6 at a Mach number of 1.12.

CORRECTIONS

The usual corrections to the Mach number and dynamic pressure for the effects of model and wake blockage and the drag coefficient for the effect of the pressure gradient caused by the wake are no longer necessary with the use of longitudinal slots in the test section (reference 3).

The drag data have been corrected for base pressure such that the drag corresponds to conditions where the body base pressure is equal to the free-stream static pressure.

No corrections for wing twist owing to bending of the swept wings have been applied to the data. Since the wings were constructed of steel, however, it is believed that bending did not materially change the aerodynamic characteristics of the data presented herein.

There exists a range of Mach numbers above Mach number 1.0 where the data are affected by reflected shock waves. On the basis of unpublished studies, it was estimated that the reflected nose shock wave should clear the rear of the model at Mach numbers above 1.08. Schlieren pictures made during the tests have substantiated these calculations. The unpublished results of tests made in the Langley 8-foot high-speed tunnel also indicate that although a detached bow wave exists on the model at low supersonic Mach numbers the reflected wave up to a Mach number of approximately 1.04 is of such weak intensity that the data are

[redacted]

unaffected. Accordingly, no data were taken in the range of Mach numbers from 1.04 to 1.08; and in the final cross plots of the results the curves are shown as dashed lines in this range of Mach numbers.

RESULTS AND DISCUSSION

An index of the figures presenting the results is as follows:

Force and moment characteristics:	Figure
α, C_D, and C_m plotted against C_L for wing 1	6
α, C_D, and C_m plotted against C_L for wing 2	7
α, C_D, and C_m plotted against C_L for wing 3	8
α, C_D, and C_m plotted against C_L for wing 4	9
C_{L_α} plotted against M	10
C_{D_o} plotted against M	11
dC_D/dC_L^2 plotted against M	12
$(L/D)_{max}$ plotted against M	13
$C_{L_{(L/D)_{max}}}$ plotted against M	14
dC_m/dC_L plotted against M	15
C_L, C_D, and C_m plotted against α for body	16

The reference axes of the data presented in the figures have been changed from body axes to wind axes. In order to facilitate presentation of the data, staggered scales have been used in many of the figures and care should be taken in identifying the zero axis for each curve. All references to wings in this discussion refer to data presented for wing-body configurations.

Lift Characteristics

The lift-curve slopes for the four wing-body configurations are presented as functions of Mach number at lift coefficients of 0 and 0.3 in figure 10. At zero lift, the results indicated that decreasing the thickness ratio of the wings increased the Mach number at which the lift-curve slopes started to decrease. For wings 1, 2, and 3, the slopes decreased at Mach numbers of 0.975, 0.955, and 0.940, respectively. The results also indicated that the lift-curve slopes at zero lift for wings 1, 2, and 3 increased 69 percent, 59 percent, and 42 percent, respectively, with increasing Mach number up to the force-break Mach number.

[redacted]

At a lift coefficient of 0.3, the lift-curve slopes for wings 1, 2, and 3 exhibited similar trends as at a lift coefficient of 0 except that the increase in C_{L_α} at high subsonic Mach numbers was generally less.

There are appreciable structural advantages in using a wing with thickened root sections which make it attractive from a design standpoint; however, its use depends upon whether or not it adversely affects the aerodynamic characteristics, particularly in the transonic speed range, when compared with a wing of constant spanwise thickness. A comparison of wing 4 with wing 2 in figure 10 shows that gradually thickening the root sections on wing 4 from 6 percent at the 0.40-semispan station to 12 percent at the plane of symmetry did not appreciably change the lift-curve slope values throughout the Mach number range, indicating that the lift characteristics of wing 4 were as good as those of wing 2.

Drag Characteristics

The effects of thickness ratio and Mach number on the drag at zero lift for wings 1, 2, and 3 are shown in figure 11. Reducing the thickness ratio from 9 percent for wing 3 to 4 percent for wing 1 resulted in an increase in the drag rise Mach number from 0.925 to 0.975. At subsonic Mach numbers below the force break, wing 3 had a value of drag which was approximately 16 percent lower than wings 1 and 2. Although the reasons for this are not clear, it is believed that wing 3 had a more favorable pressure gradient existing over the airfoil surface, resulting in a greater region of laminar flow and therefore lower drag. It is also possible that the surface on wing 2 may not have been entirely aerodynamically smooth, owing to removable plates which were used for attaching various nacelles to the wing, which might account for the fact that wing 2 had higher values of drag at subsonic Mach numbers than either wing 1 or wing 3. At a supersonic Mach number of 1.10, however, the drag increased approximately by a factor of 4, compared with the low-speed value, for wing 3. For the 6- and 4-percent-thick wings, the drag coefficients increased by factors of about 2.4 and 2.0, respectively, for similar Mach numbers.

A comparison of wing 4 with wing 2 in figure 11 shows the effect of the thickened inboard sections on the drag at zero lift. The thickened-root wing (wing 4) had a low-speed value of drag which was approximately 19 percent lower than that for wing 2, possibly for reasons similar to those given for wing 3. The thickened-root wing, however, decreased the drag rise Mach number from 0.975 to 0.95 and increased the drag at a Mach number of 1.10 by 22 percent. When compared with wing 3, on the other hand, the drag for wing 4 at a Mach number of 1.10 was approximately 14 percent lower.

[redacted]

Figure 12 shows the effect of wing thickness ratio and the thickened inboard section on drag due to lift for the four wings investigated. Generally, reducing the wing thickness did not appreciably change the value of the drag due to lift at a lift coefficient of 0.3. The drag due to lift began to rise at a Mach number of 0.90 and increased approximately 30 percent above the low-speed value at a Mach number of 1.10.

The effects of wing thickness ratio on the maximum lift-drag ratio are shown in figure 13. A comparison of the lift-drag ratios for wings 1, 2, and 3 indicated that a reduction in thickness ratio from 9 percent to 4 percent caused an increase from 0.89 to 0.925 in the Mach number for which the maximum lift-drag ratio began to decrease. This increase in Mach number at which the force break occurred would be expected since reducing the thickness ratio increased the Mach number at which the drag started to rise (fig. 11) and also increased the Mach number at which the lift-curve slopes started decreasing (fig. 10). A comparison of the $(L/D)_{max}$ values at a Mach number of 0.925 indicated that reducing the wing thickness ratio from 9 to 6 to 4 percent resulted in an increase in the $(L/D)_{max}$ value from 15.0 for wing 3 to 18.3 for wing 2, and to 25.0 for wing 1. At a Mach number of 1.10, decreasing the wing thickness ratio from 9 to 4 percent increased the $(L/D)_{max}$ value by a factor of 1.7.

The effects of tapering the wing thickness from 6 percent at the 40-percent spanwise station to 12 percent at the plane of symmetry on the maximum lift-drag ratio values are also shown in figure 13. Thickening the root section had a negligible effect on $(L/D)_{max}$ up to a Mach number of 0.95. At a Mach number of 1.10, however, the thickening of the root section caused a 16-percent decrease in $(L/D)_{max}$.

In conjunction with the maximum lift-drag ratio plots, the values of lift coefficient at which the maximum lift-drag ratio occurred are presented as a function of Mach number in figure 14. Reducing the wing thickness ratio was effective in reducing the positive shift in lift coefficient for $(L/D)_{max}$ as the Mach number increased from 0.70 to 1.10. As an example, the shift in the lift coefficient for $(L/D)_{max}$ for wing 1 was approximately 40 percent as compared with 63 percent for wing 3.

Pitching-Moment Characteristics

In general, the pitching-moment curves for Mach numbers up to 0.925 (figs. 6(c), 7(c), 8(c), 9(c)) showed pronounced unstable breaks near a lift coefficient of 0.6 for the four wing-body configurations. As the Mach number increased beyond 0.95, however, the break became less sharp.

The effects of Mach number on the static-longitudinal-stability parameter dC_m/dC_L for the four wings are presented in figure 15. As the Mach number was increased from 0.50 to 1.10 for zero lift, the aerodynamic center for the 9-percent-thick wing moved rearward 11.0 percent as compared to a 15-percent-rearward movement of the aerodynamic center for the 4- and 6-percent-thick wings. Through the transonic speed range, there was probably an outboard movement of the boundary layer (reference 4) which resulted in a more pronounced separation at the tip for the 9-percent-thick wing than for either the 4- or 6-percent-thick wings. This increase in flow separation for the 9-percent-thick wing would prevent the aerodynamic center from moving as far rearward as the aerodynamic center for either the 4- or 6-percent-thick wing.

Figure 15 also shows that at 0 and 0.3 lift coefficients, the thickened inboard sections of wing 4 did not appreciably change the location of the aerodynamic center as compared to the location of the aerodynamic center for wing 2.

Body-Alone Characteristics

In figure 16 are presented body-alone data, by means of which combined wing-plus-wing-body-interference data may be obtained from comparisons with the wing-body configurations. It can be seen that the effects of compressibility on the lift and pitching-moment coefficients are negligible. At 0° angle of attack, the low-speed drag coefficient of the body based on the wing area increased from a value of 0.0030 to 0.0062 as the Mach number increased to 1.10.

SUMMARY OF RESULTS

The results of an investigation of a wing of aspect ratio 3.5, taper ratio 0.2, 47° sweepback of the quarter-chord line, and varying only in thickness ratio and spanwise thickness distribution indicated the following:

1. In general, reducing the wing thickness ratio from 9 percent to 4 percent was effective in increasing:

   (a) The lift-curve break Mach number from 0.940 to 0.975 at zero lift

   (b) The drag rise Mach number from 0.925 to 0.975 at zero lift

   (c) The Mach number from 0.89 to 0.925 where the maximum lift-drag ratio decreased

[redacted]

2. A large increase in the lift-curve slope at high subsonic Mach numbers was noted for the 4-percent-thick wing at zero lift. At a lift coefficient of 0.3, the lift-curve slopes for wings 4, 6, and 9 percent thick exhibited similar trends as at a lift coefficient of 0 except that the increases in lift-curve slopes at high subsonic Mach numbers were generally less.

3. At a supersonic Mach number of 1.10, the drag increased approximately by a factor of 4 above the low-speed value for the 9-percent-thick wing. For the 6- and 4-percent-thick wings, the drag coefficients increased by factors of about 2.4 and 2.0, respectively, for similar Mach numbers.

4. A comparison of the values of maximum lift-drag ratios $(L/D)_{max}$ at a Mach number of 0.925 indicated that reducing the wing thickness ratios resulted in an increase in the $(L/D)_{max}$ values from 15.0 for the 9-percent-thick wing to 18.3 for the 6-percent-thick wing, and to 25.0 for the 4-percent-thick wing. At a Mach number of 1.10, decreasing the wing thickness ratio from 9 to 4 percent increased the $(L/D)_{max}$ value by a factor of 1.7.

5. As the Mach number increased from 0.50 to 1.10, the aerodynamic center for the 9-percent-thick wing moved rearward 11 percent as compared with a 15-percent rearward movement for the 4- and 6-percent-thick wings.

6. The characteristics of the 6-percent-thick wing with the thickened inboard sections were approximately intermediate between those of the 6- and 9-percent-thick wings.

Langley Aeronautical Laboratory
National Advisory Committee for Aeronautics
Langley Field, Va.

REFERENCES

1. Wright, Ray H., and Ritchie, Virgil S.: Characteristics of a Transonic Test Section with Various Slot Shapes in the Langley 8-Foot High-Speed Tunnel. NACA RM L51H10, 1951.

2. Osborne, Robert S.: A Transonic-Wing Investigation in the Langley 8-Foot High-Speed Tunnel at High Subsonic Mach Numbers and at a Mach Number of 1.2. Wing-Fuselage Configuration Having a Wing of 45° Sweepback, Aspect Ratio 4, Taper Ratio 0.6, and NACA 65A006 Airfoil Section. NACA RM L50H08, 1950.

3. Wright, Ray H., and Ward, Vernon G.: NACA Transonic Wind-Tunnel Test Sections. NACA RM L8J06, 1948.

4. Whitcomb, Richard T.: An Experimental Study at Moderate and High Subsonic Speeds of the Flow over Wings with 30° and 45° of Sweepback in Conjunction with a Fuselage. NACA RM L50K27, 1951.

TABLE I

AIRFOIL COORDINATES FOR THE FOUR WING-BODY CONFIGURATIONS

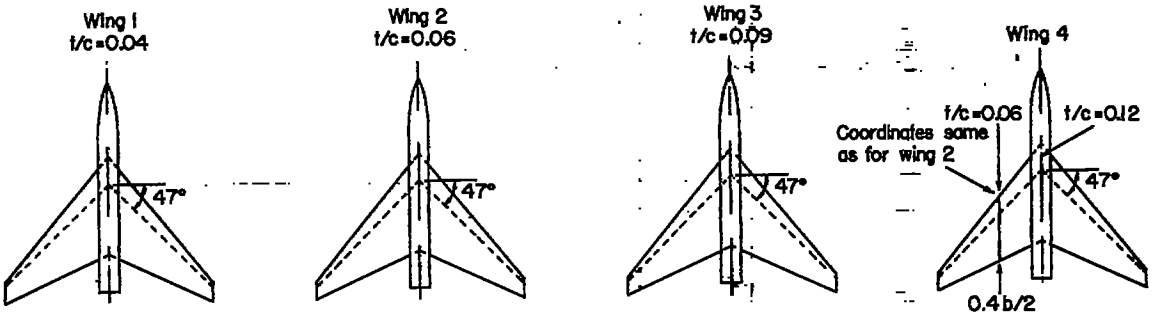

COORDINATES

x/c	y/c upper surface	y/c lower surface
0	0	0
.5	.411	.245
.75	.499	.271
1.25	.665	.289
2.5	.962	.324
5.0	1.435	.367
7.5	1.776	.429
10	2.039	.472
15	2.423	.577
20	2.642	.682
25	2.800	.787
30	2.887	.892
35	2.983	.997
40	2.992	1.006
45	2.940	1.011
50	2.852	1.006
55	2.712	.945
60	2.511	.857
65	2.265	.761
70	1.986	.674
75	1.680	.577
80	1.356	.481
85	1.041	.385
90	.726	.289
95	.402	.201
100	.105	.105
Tangent point	60.00	60.00

L.E. radius = 0.0016c

x/c	y/c upper surface	y/c lower surface
0	0.061	0
.5	.577	.376
.75	.717	.446
1.25	.919	.534
2.5	1.304	.621
5.0	1.872	.761
7.5	2.318	.857
10	2.668	.980
15	3.150	1.269
20	3.482	1.496
25	3.701	1.697
30	3.858	1.846
35	3.946	1.960
40	3.981	2.021
45	3.934	2.030
50	3.823	1.977
55	3.613	1.872
60	3.342	1.697
65	3.018	1.487
70	2.651	1.277
75	2.231	1.059
80	1.785	.849
85	1.339	.639
90	.892	.420
95	.446	.210
100	0	0

L.E. radius = 0.0028c

x/c	y/d upper surface	y/c lower surface
0	0.156	0
.5	.846	.574
.75	1.021	.680
1.25	1.283	.846
2.5	1.789	1.069
5.0	2.537	1.400
7.5	3.111	1.662
10	3.577	1.896
15	4.244	2.352
20	4.705	2.751
25	5.045	3.052
30	5.288	3.276
35	5.415	3.441
40	5.473	3.529
45	5.424	3.519
50	5.249	3.422
55	4.967	3.208
60	4.579	2.916
65	4.102	2.566
70	3.568	2.197
75	2.975	1.837
80	2.342	1.468
85	1.689	1.098
90	1.186	.739
95	.593	.369
100	0	0

L.E. radius = 0.0056c

x/c	Root station	
	y/c upper surface	y/c lower surface
0	0.301	0
.5	1.120	.754
.75	1.335	.904
1.25	1.658	1.141
2.5	2.261	1.507
5.0	3.208	2.024
7.5	3.919	2.433
10	4.500	2.799
15	5.362	3.445
20	5.965	3.964
25	6.395	4.414
30	6.718	4.716
35	6.912	4.910
40	6.977	5.017
45	6.912	4.996
50	6.675	4.823
55	6.288	4.522
60	5.771	4.113
65	5.168	3.618
70	4.457	3.101
75	3.725	2.584
80	2.929	2.067
85	2.239	1.550
90	1.486	1.034
95	.732	.517
100	0	0

L.E. radius = 0.0099c

NACA

[redacted]

[redacted]

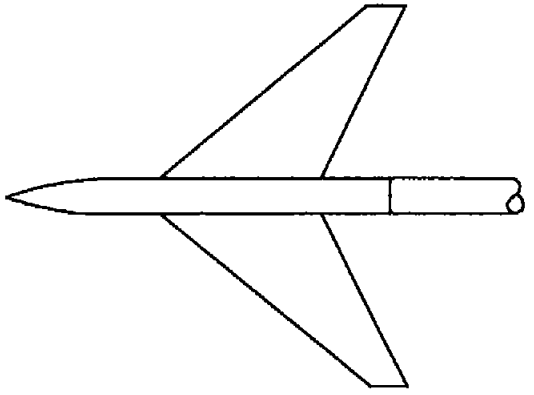

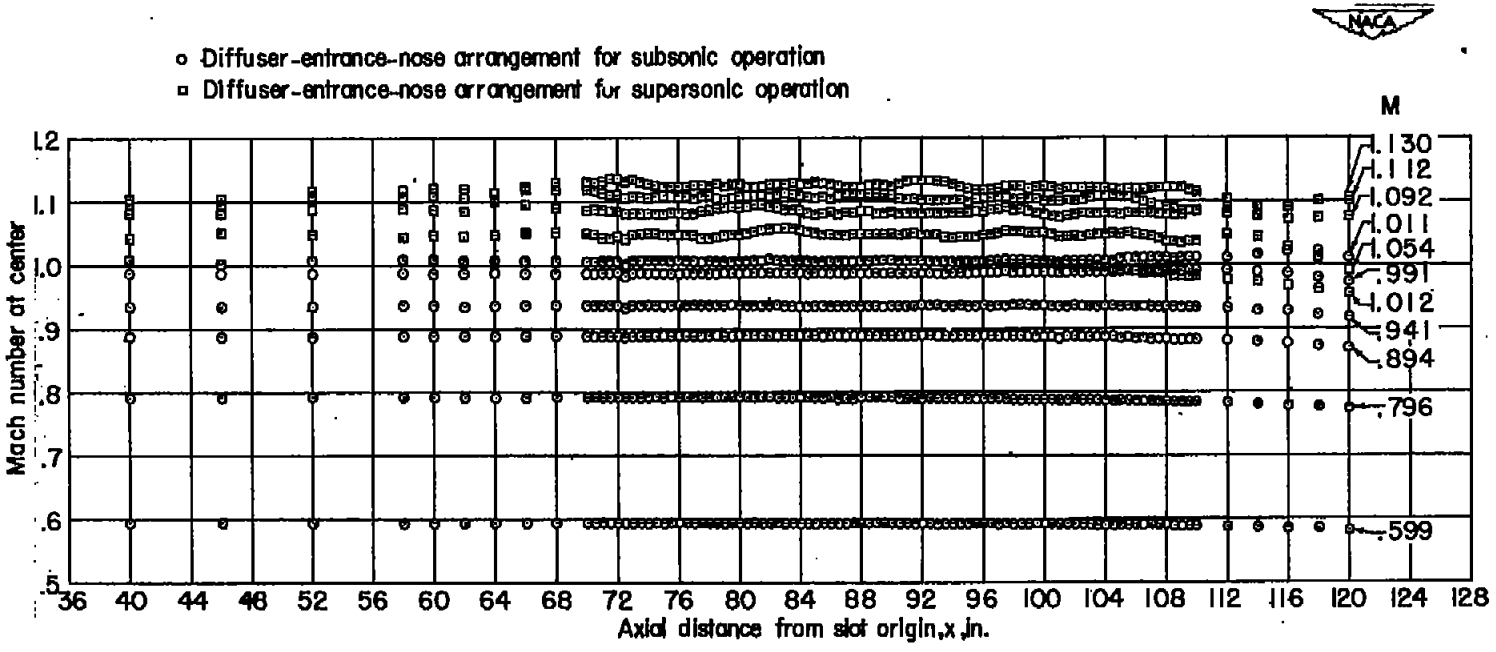

Figure 1.- Mach number distributions along the center of the test section.

Figure 2.- Photograph of model as tested in the Langley 8-foot high-speed tunnel.

Wing Details

Airfoil section parallel to plane of symmetry
Thickness distribution . . . . . NACA 65A series
Mean line ordinates . . . 1/3 of NACA 230 series + NACA 6-series uniform-load mean line (a = 1.0) for C_{l_1} = 0.1

Area, sq ft	1.143
Aspect ratio	3.5
Taper ratio	0.2
Incidence, deg	0
Dihedral, deg	0
Geometric twist, deg	0

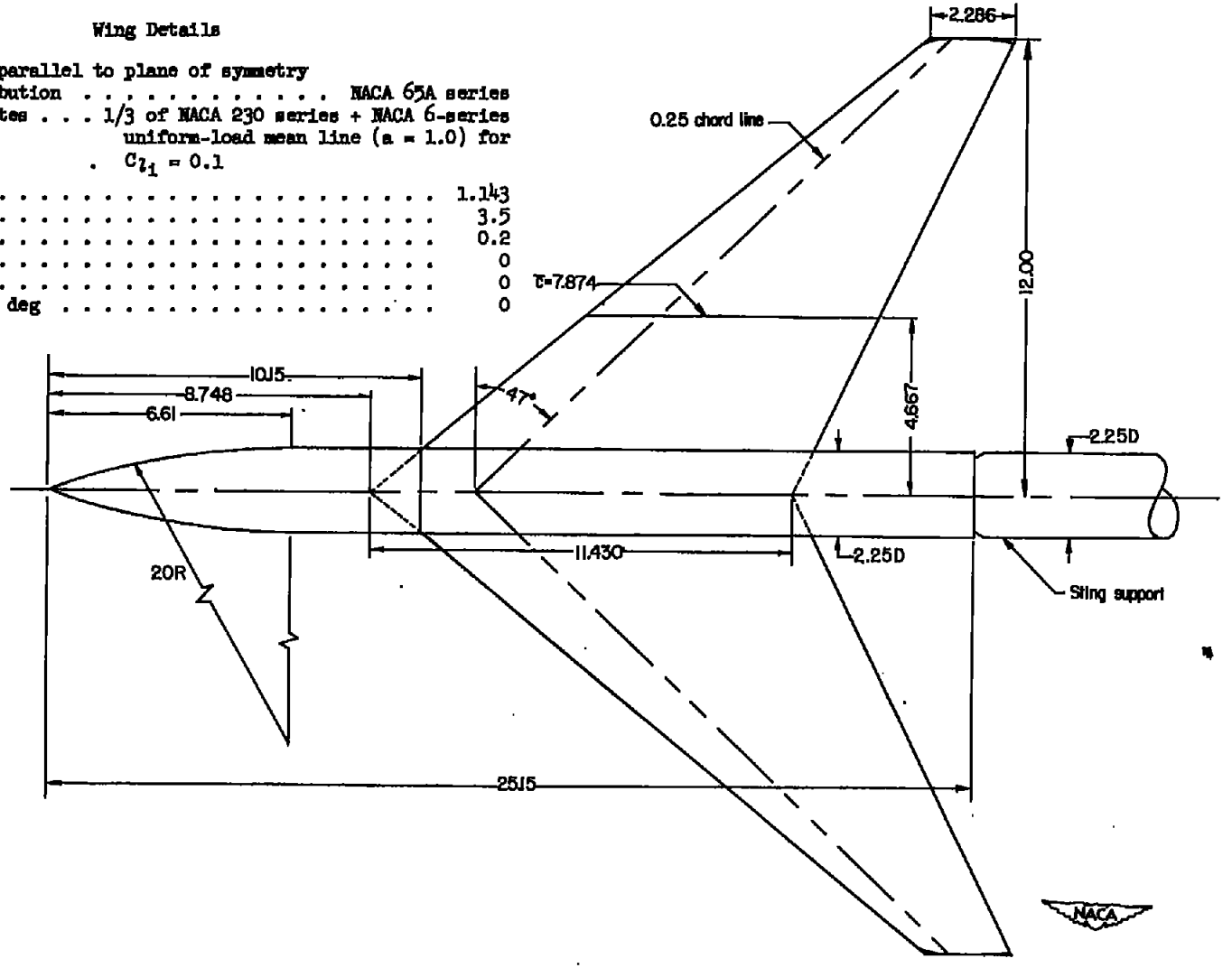

Figure 3.- Model details. All dimensions are in inches.

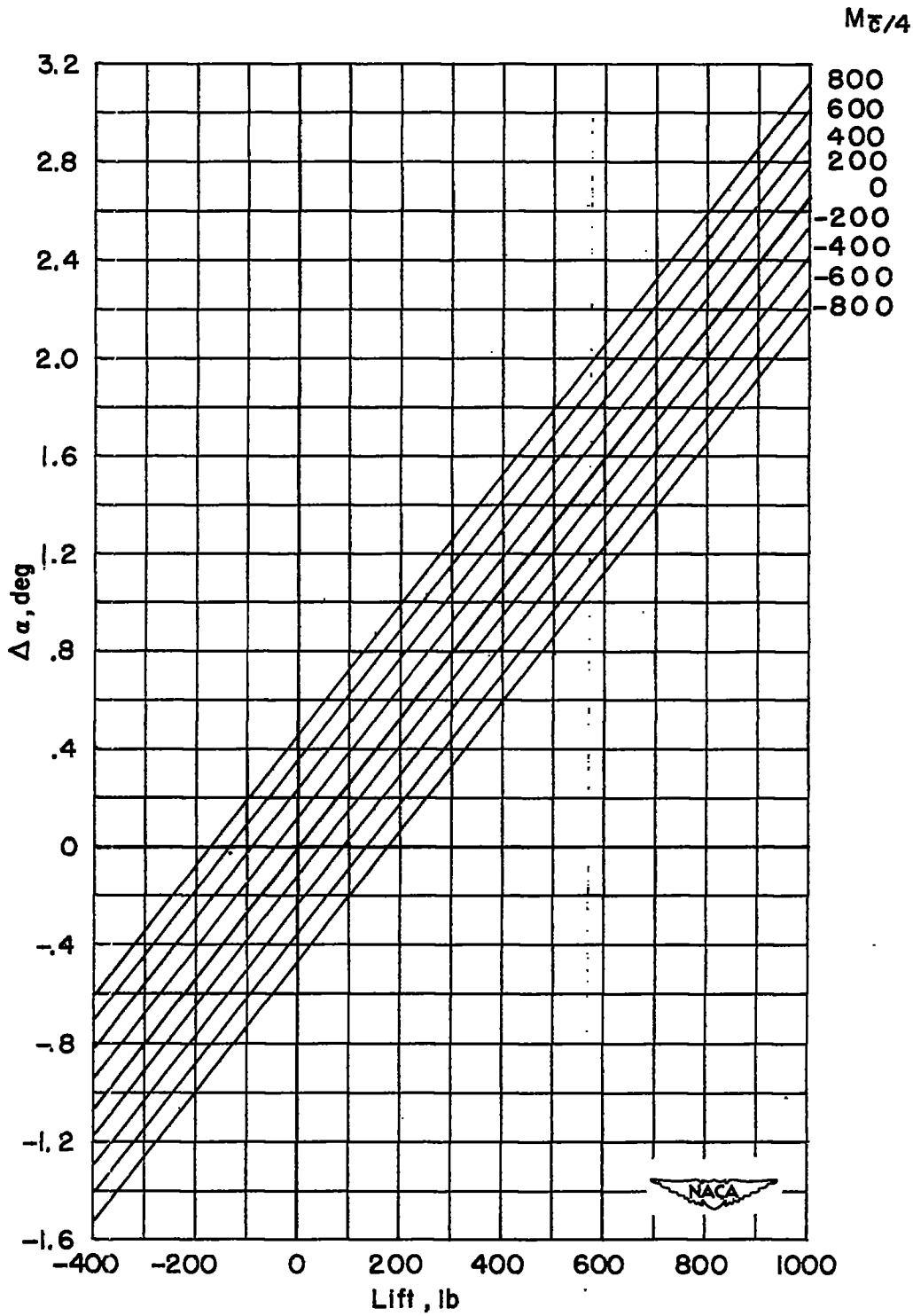

Figure 4.- Sting deflection due to lift and pitching moment.

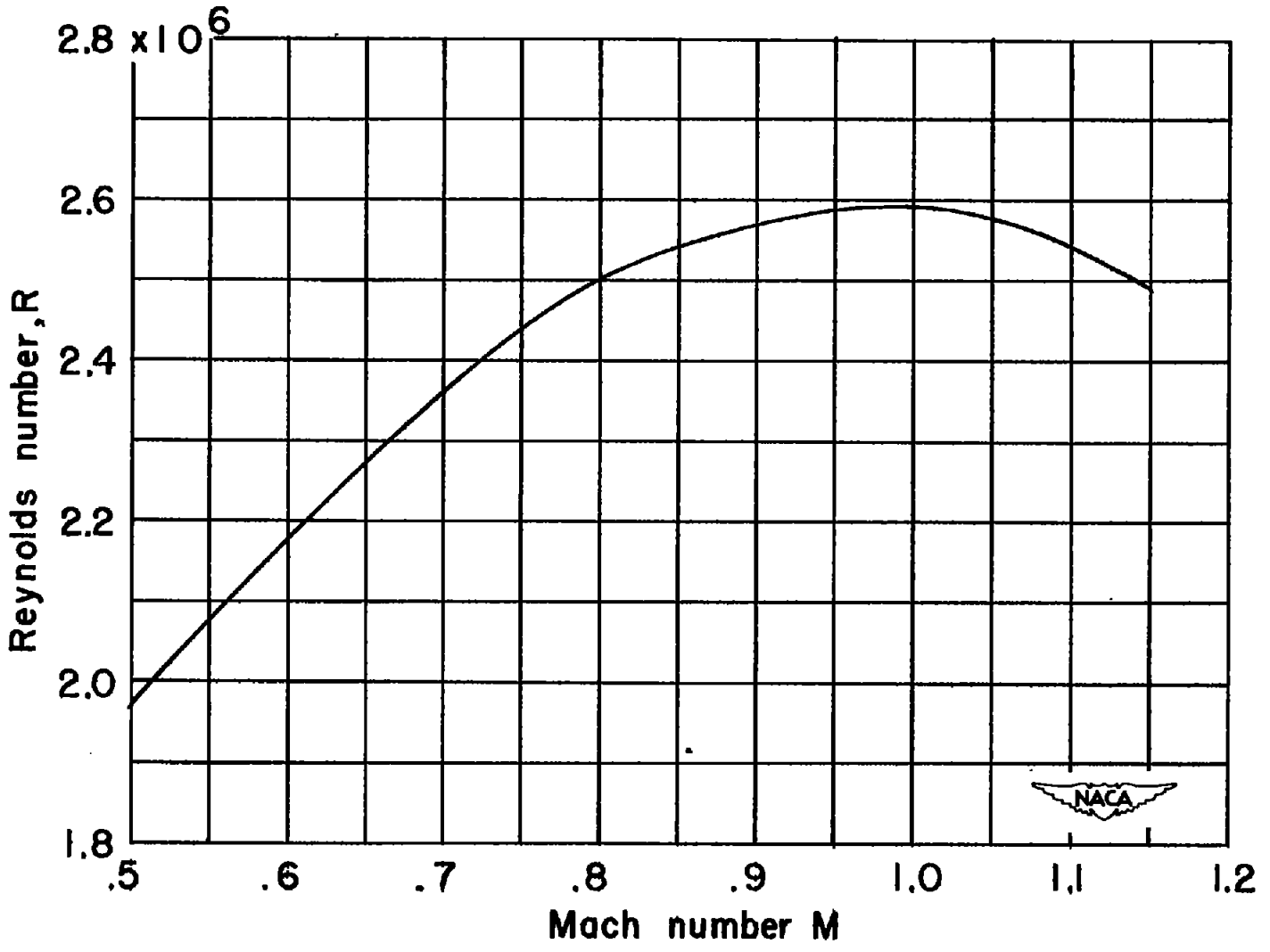

Figure 5.- Variation with Mach number of test Reynolds number based on a $\bar{c}$ of 7.874 inches.

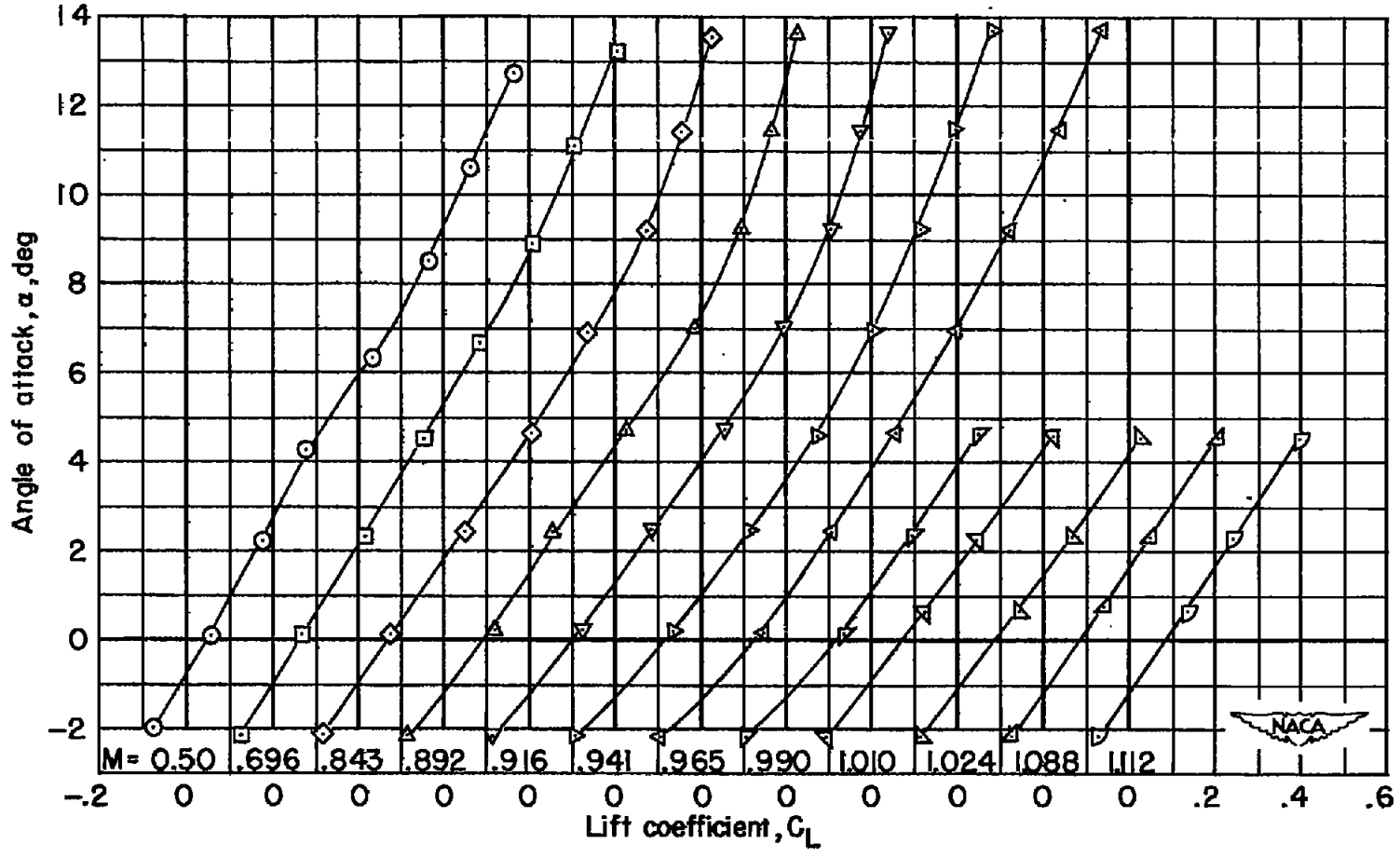

(a) Angle of attack.

Figure 6.- Variation with lift coefficient of the aerodynamic characteristics for wing 1.

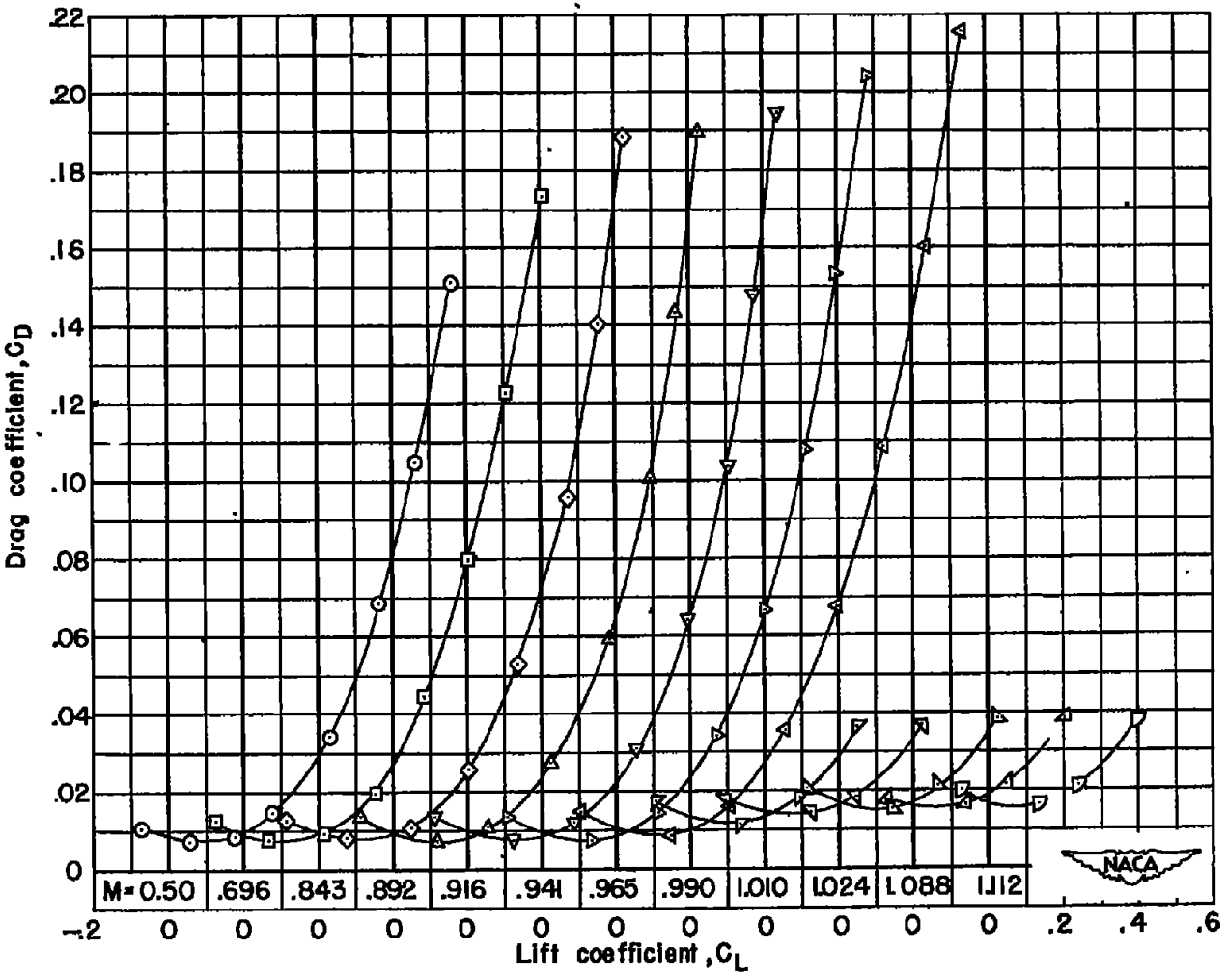

(b) Drag coefficient.

Figure 6.- Continued.

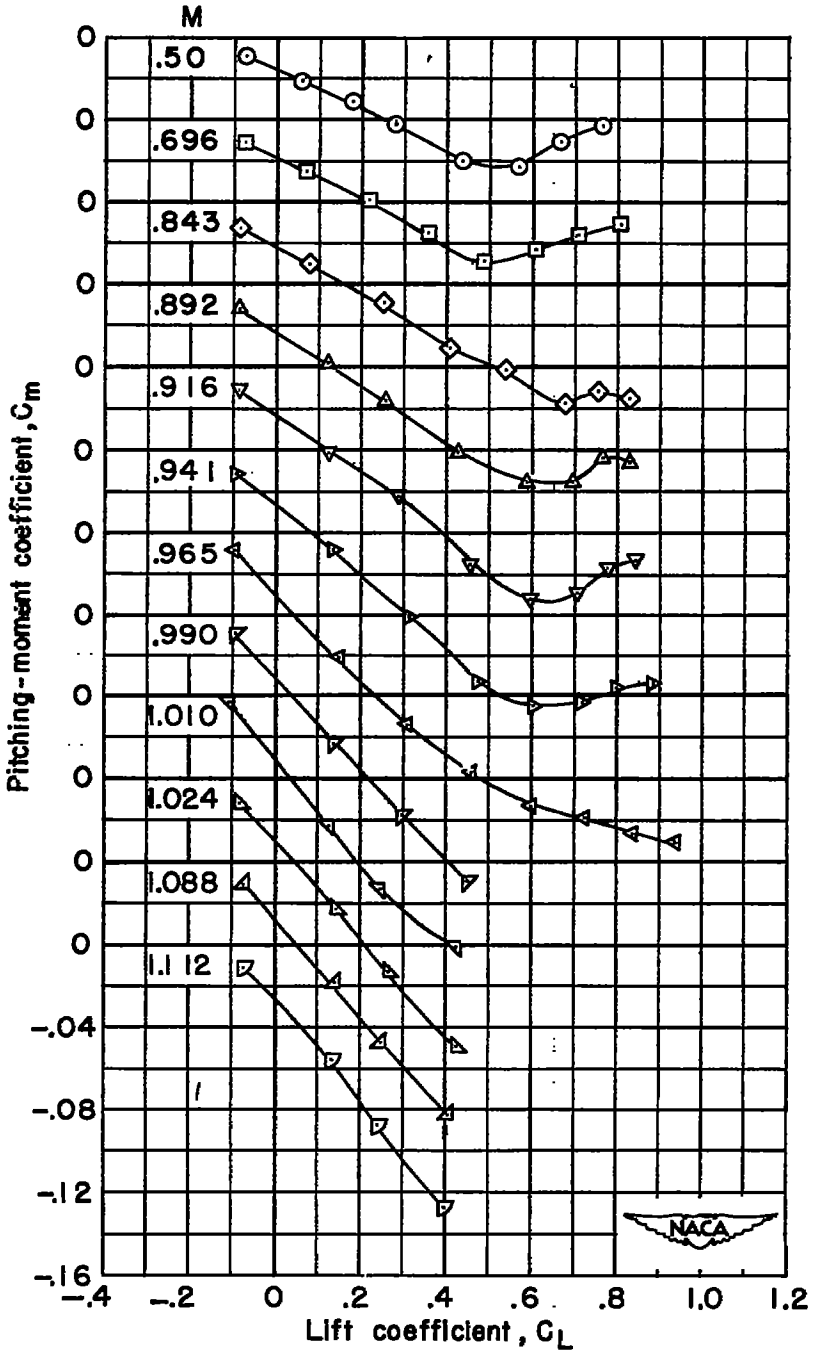

(c) Pitching-moment coefficient.

Figure 6.- Concluded.

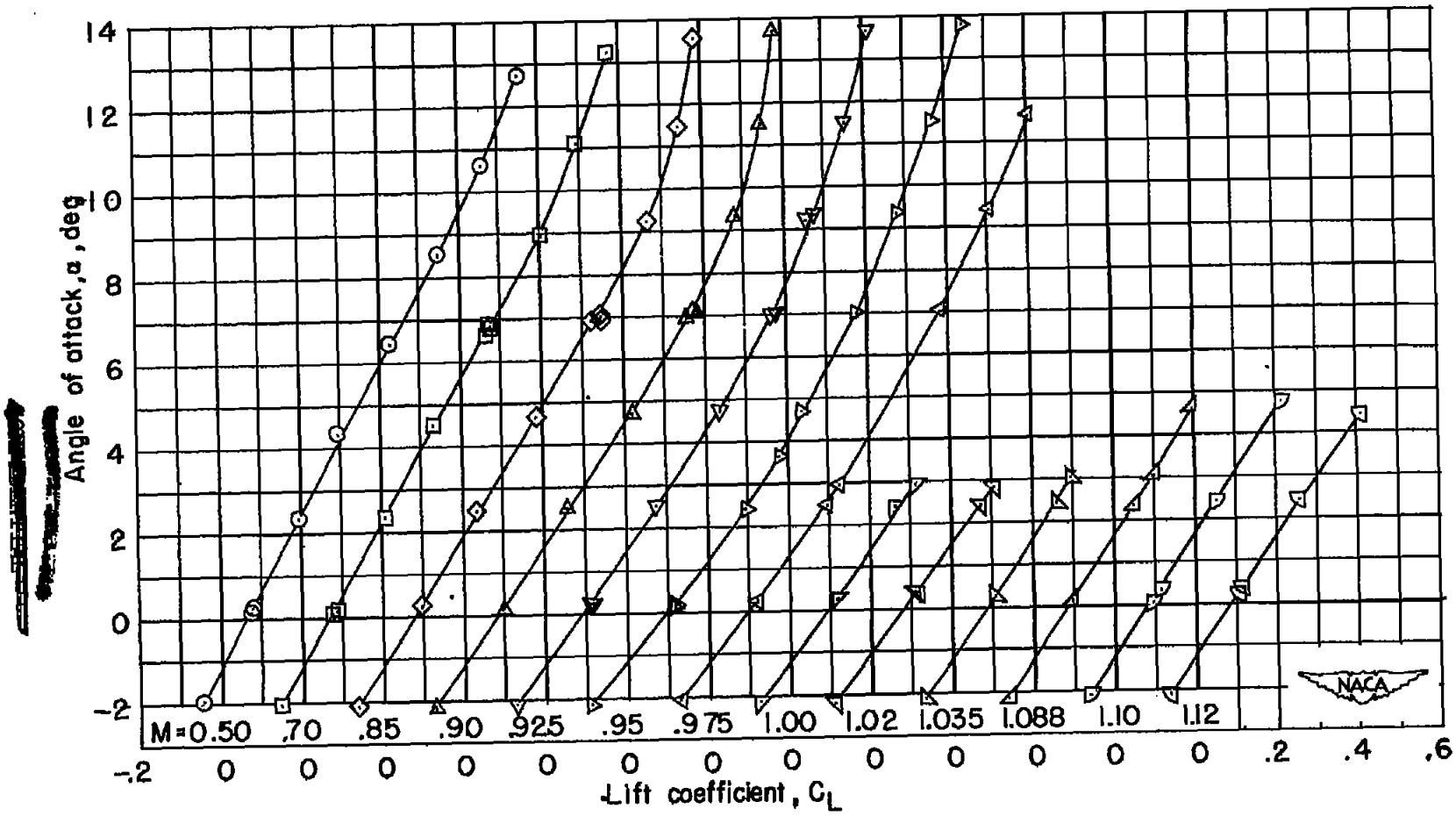

(a) Angle of attack.

Figure 7.- Variation with lift coefficient of the aerodynamic characteristics for wing 2.

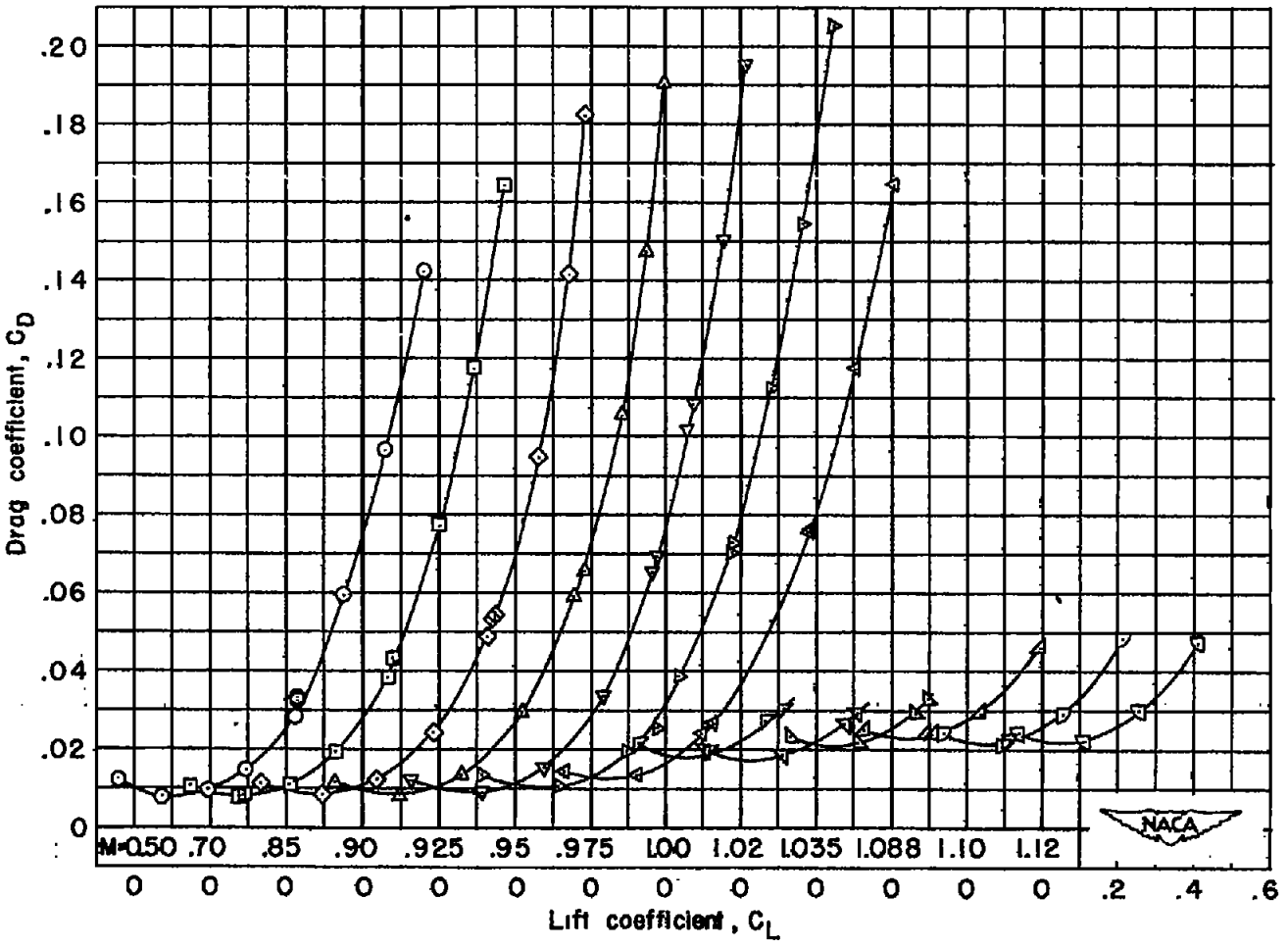

(b) Drag coefficient.

Figure 7.- Continued.

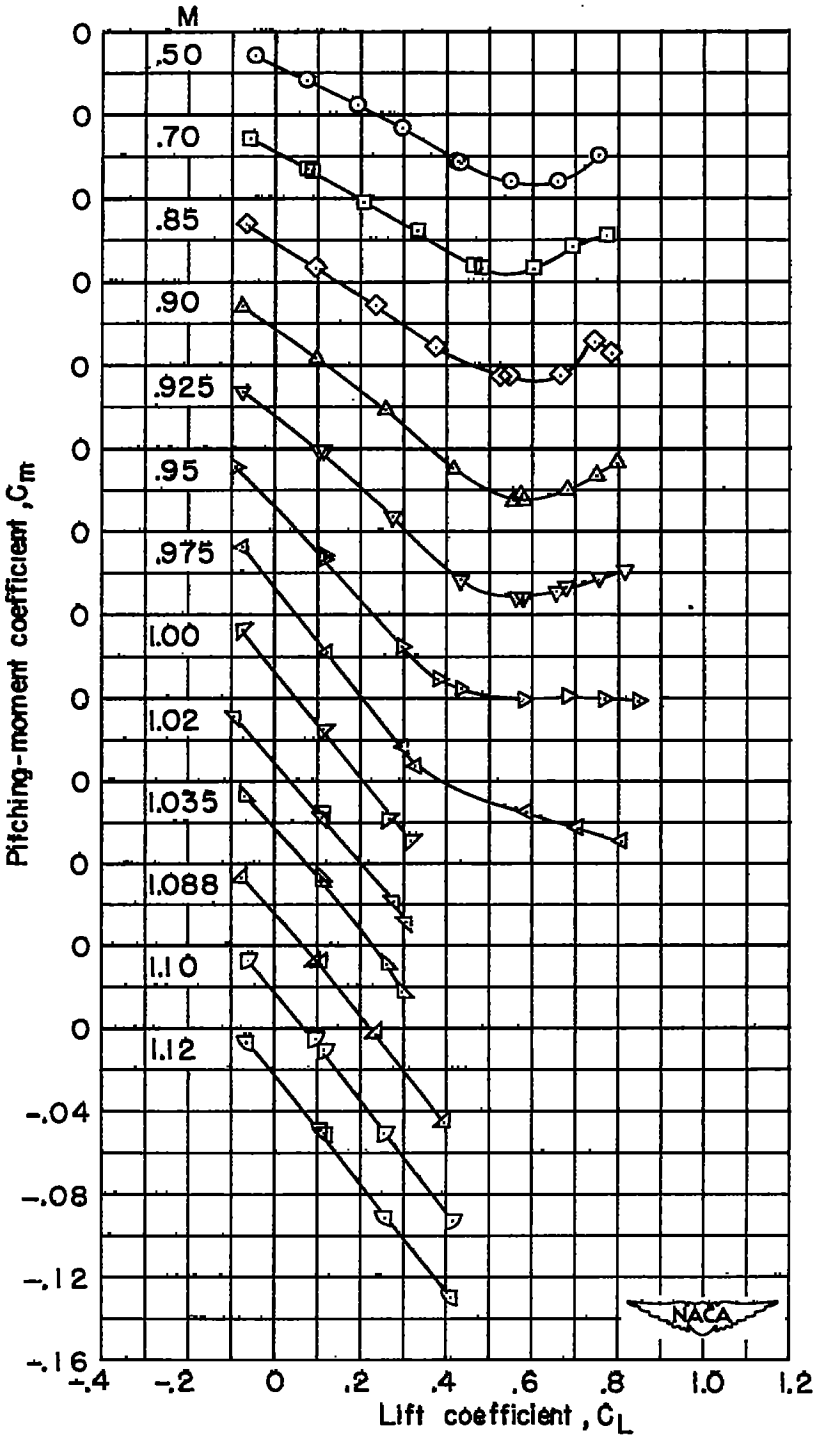

(c) Pitching-moment coefficient.

Figure 7.- Concluded.

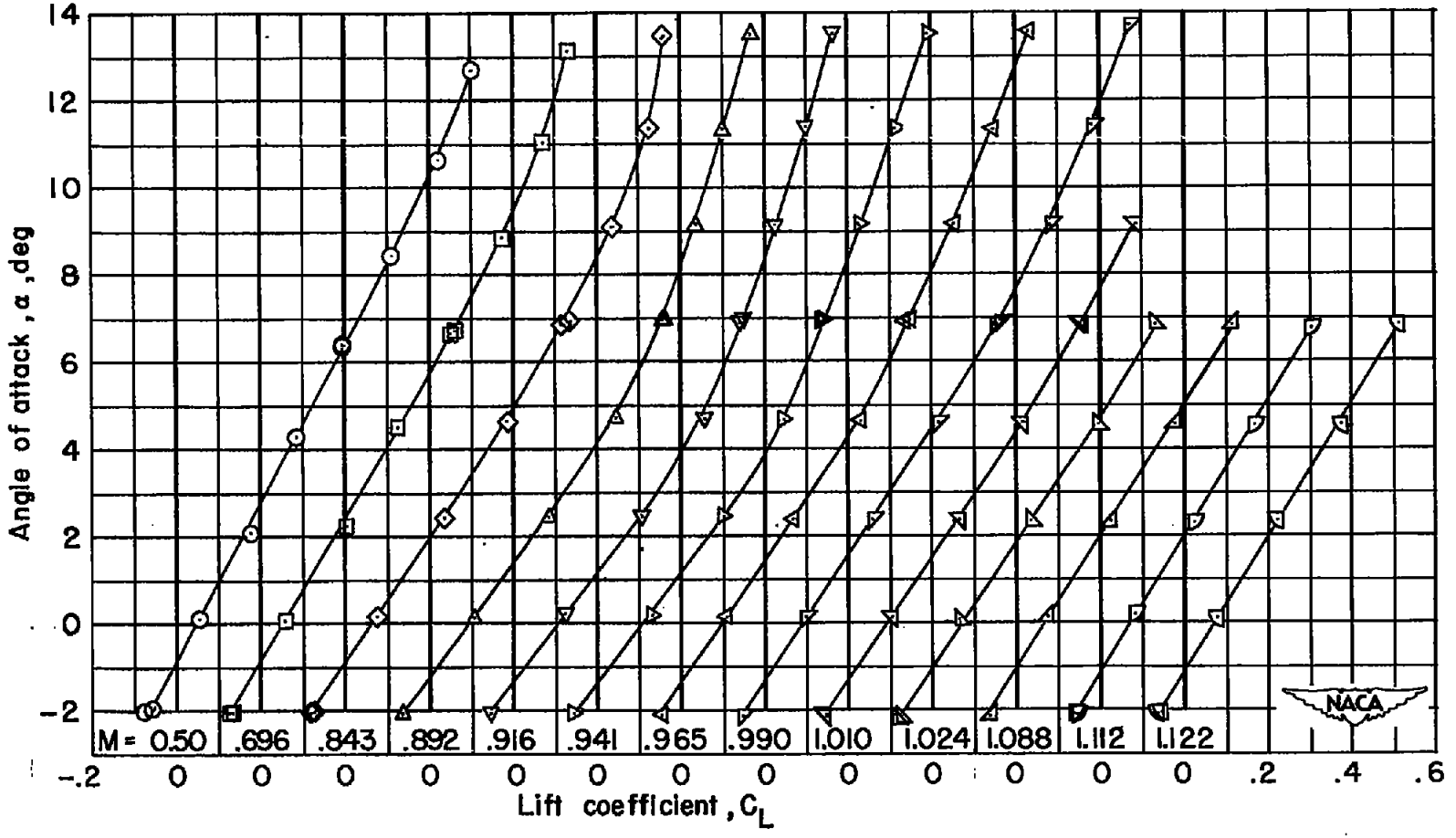

(a) Angle of attack.

Figure 8.- Variation with lift coefficient of the aerodynamic characteristics for wing 3.

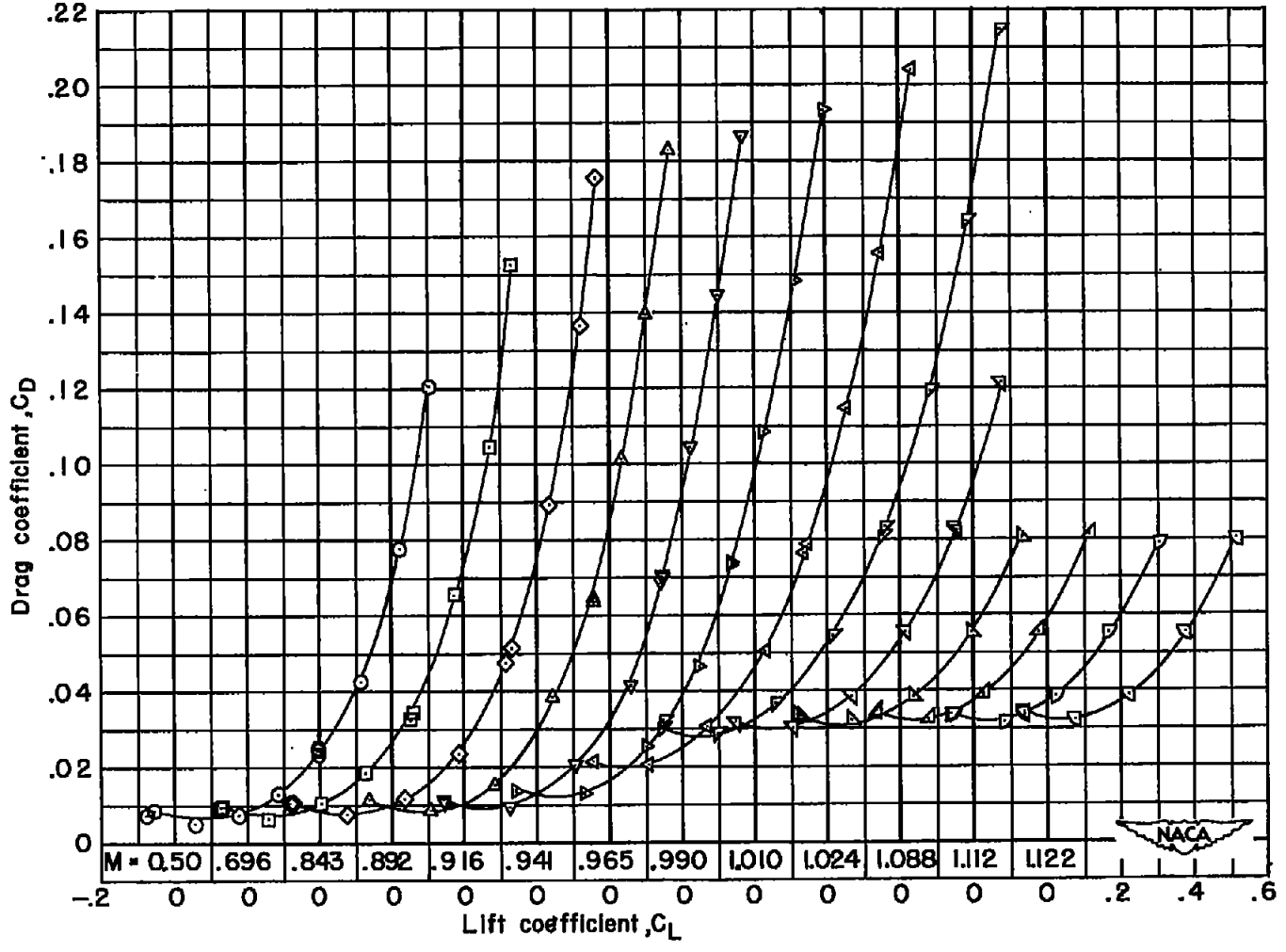

(b) Drag coefficient.

Figure 8.- Continued.

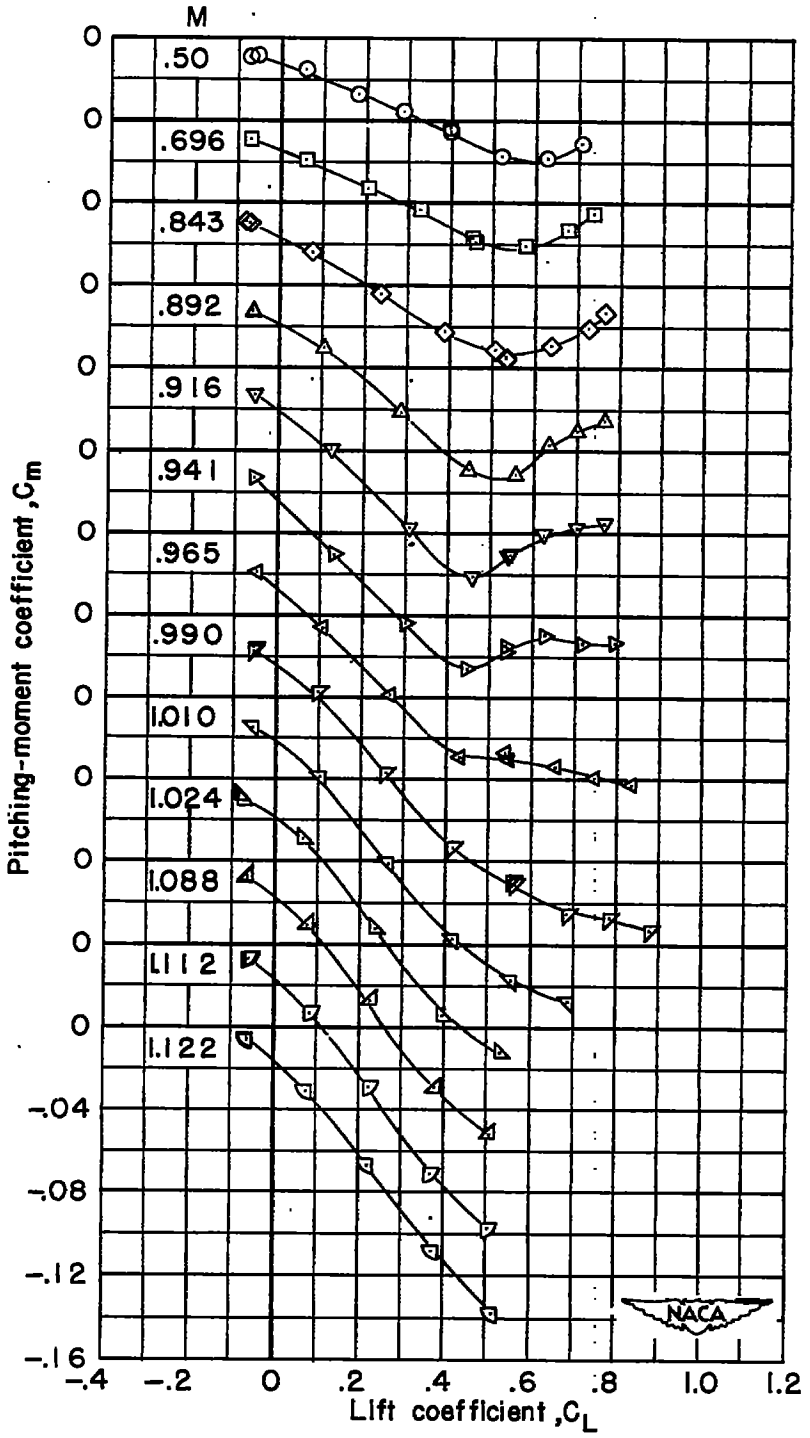

(c) Pitching-moment coefficient.

Figure 8.- Concluded.

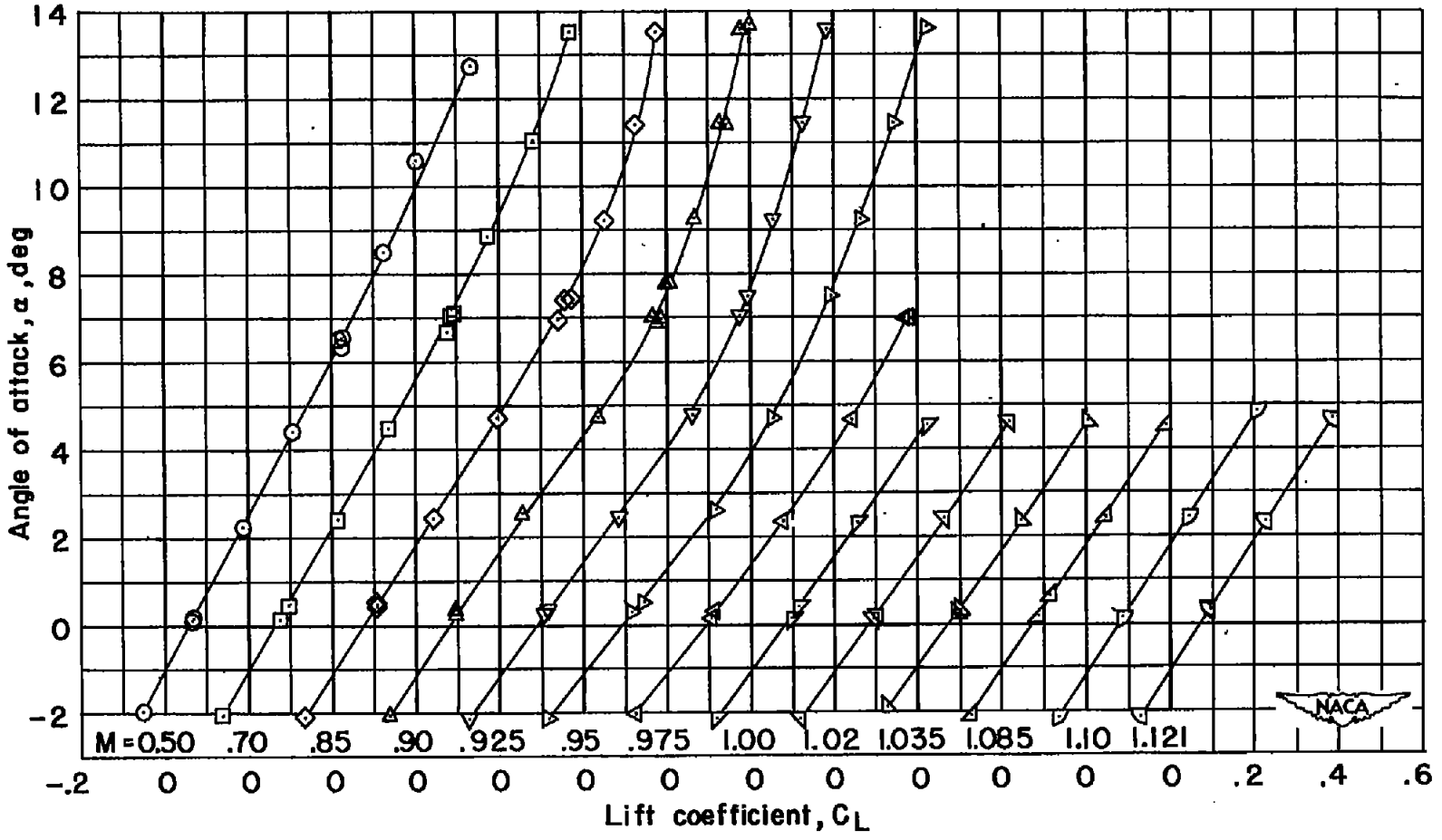

(a) Angle of attack.

Figure 9.- Variation with lift coefficient of the aerodynamic characteristics for wing 4.

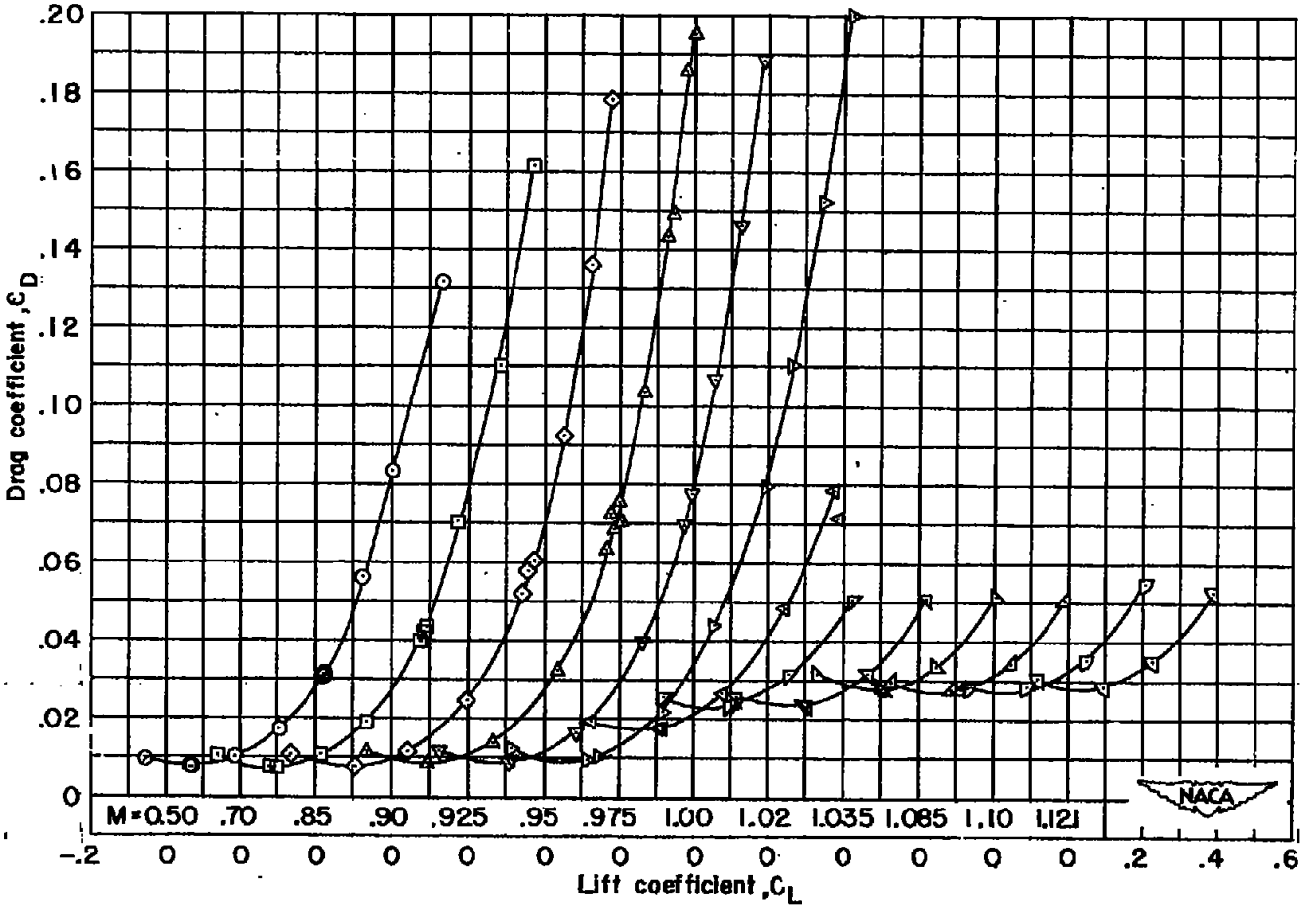

(b) Drag coefficient.

Figure 9.- Continued.

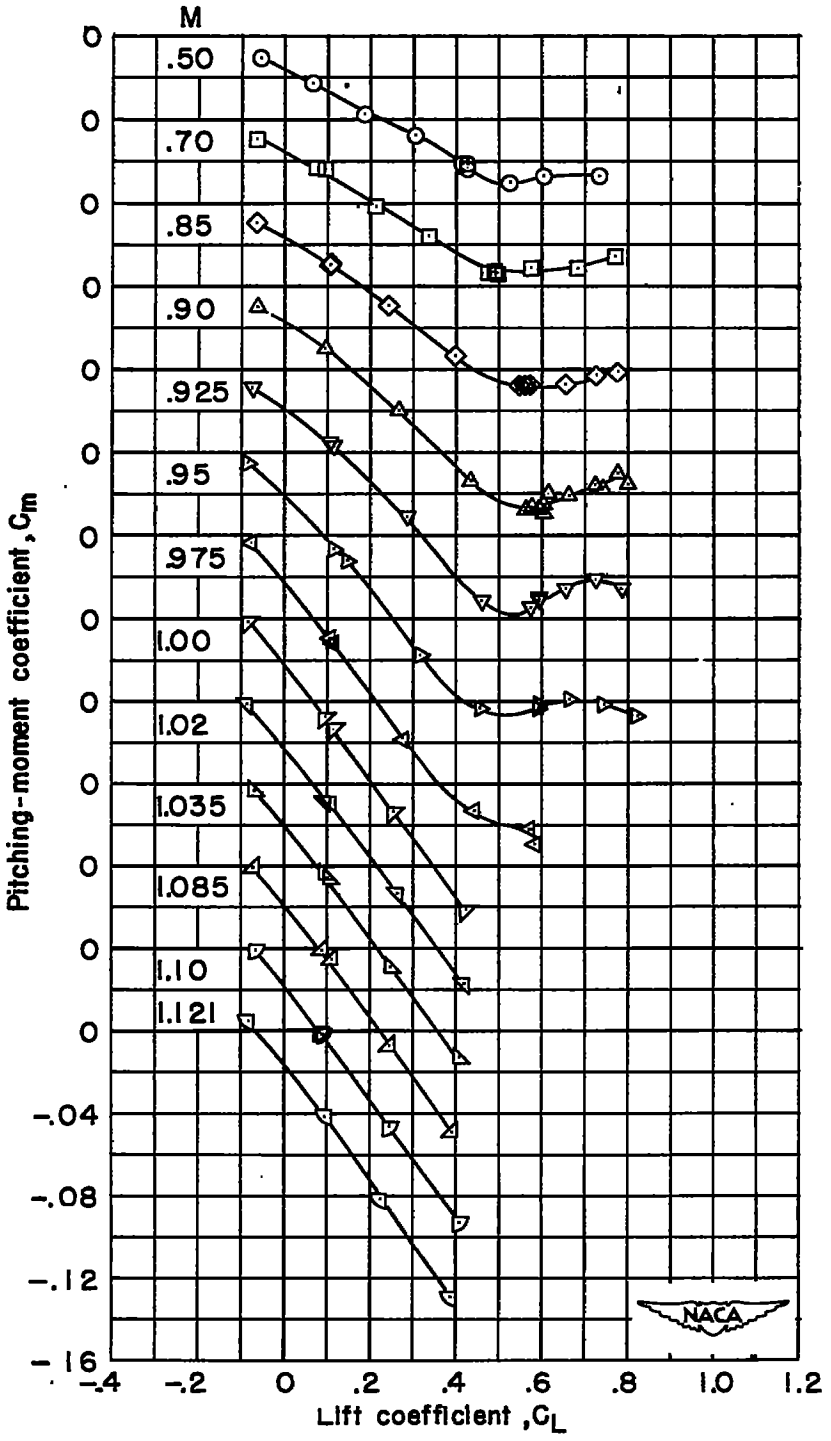

(c) Pitching-moment coefficient.

Figure 9.- Concluded.

[redacted]

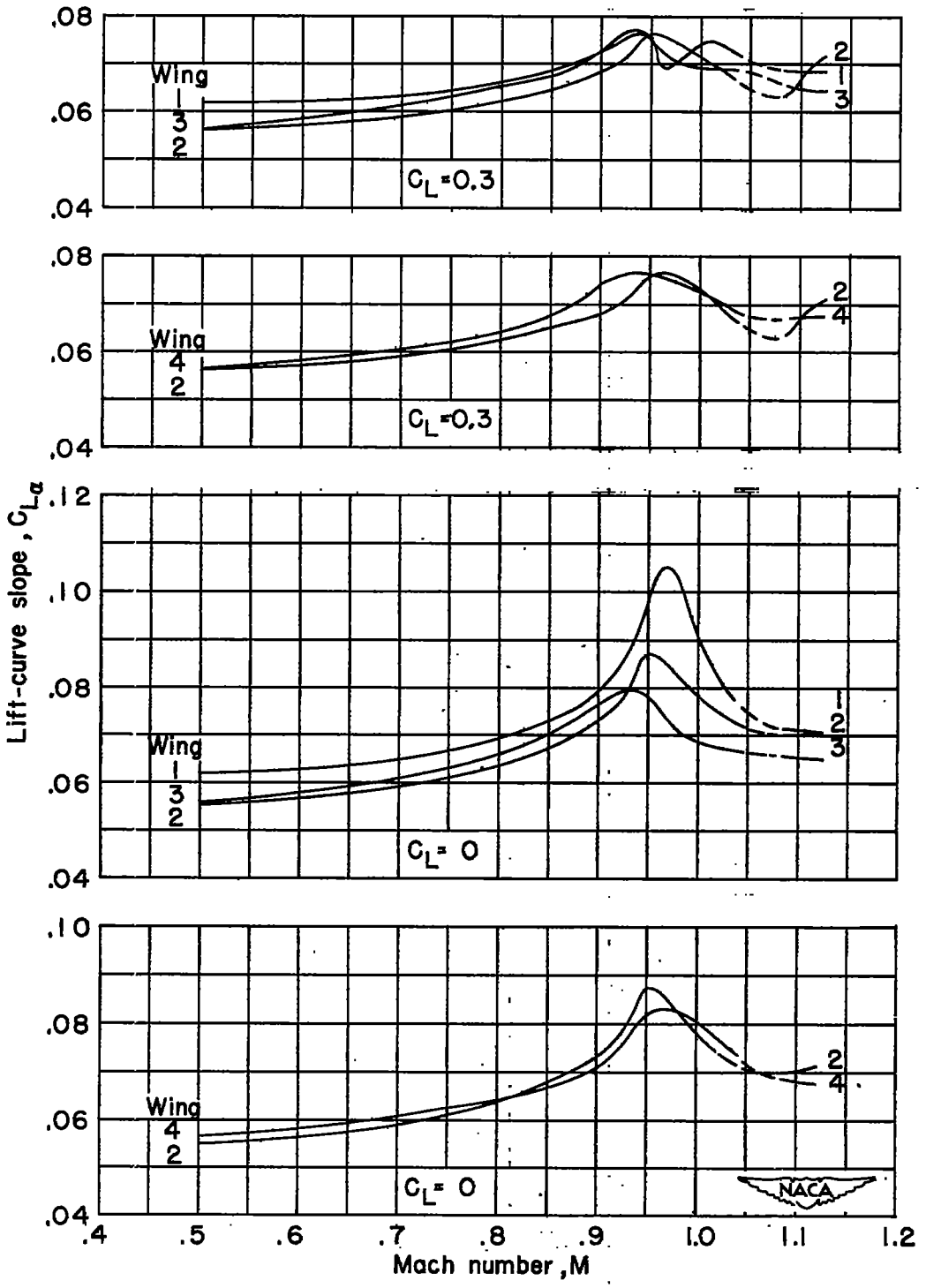

Figure 10.- Effect of thickness ratio and thickened root sections on the variation of lift-curve slope with Mach number for the wing-body configuration.

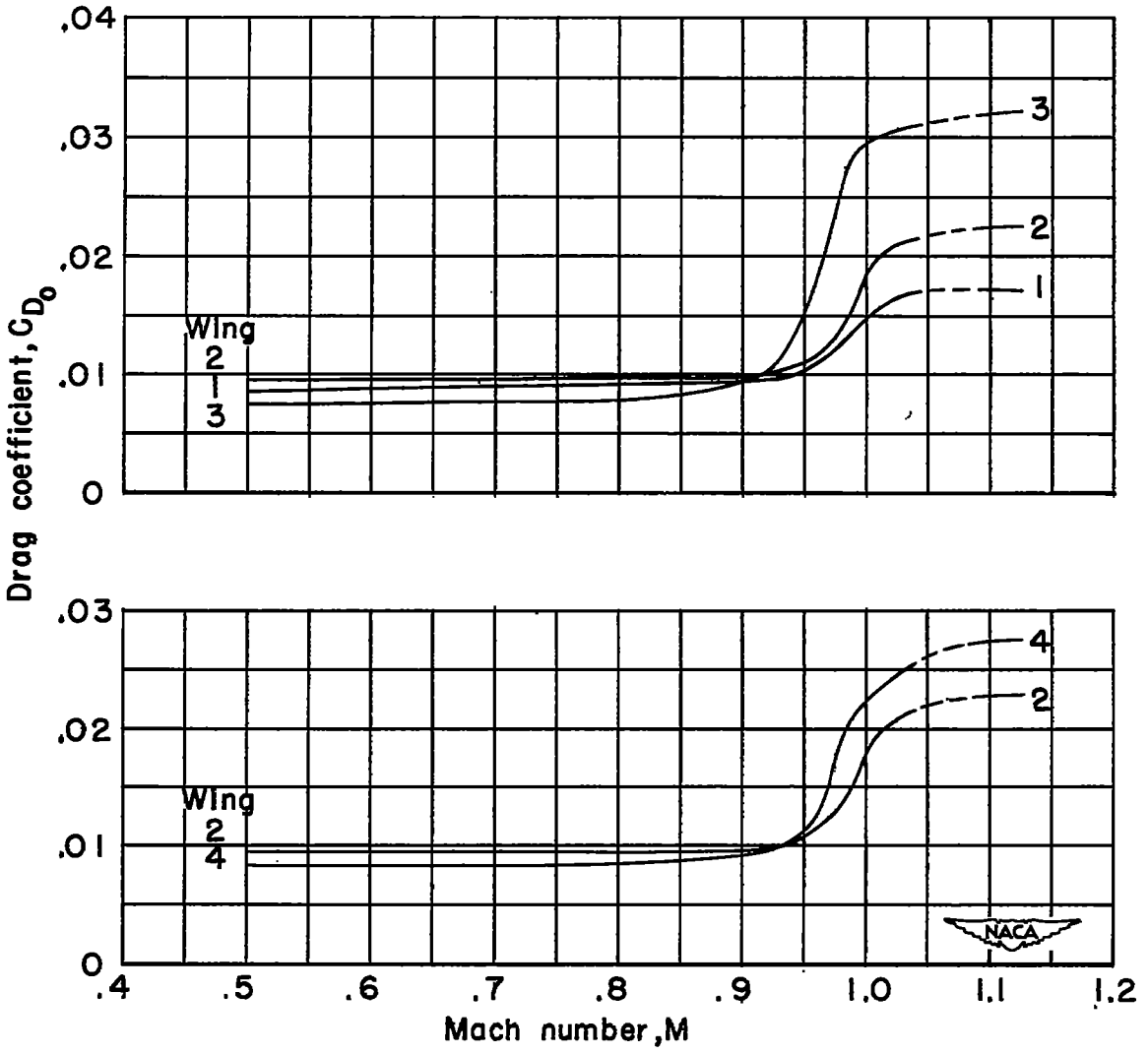

Figure 11.- Effect of thickness ratio and thickened root sections on the variation of drag coefficient at zero lift with Mach number for the wing-body configuration.

[redacted]

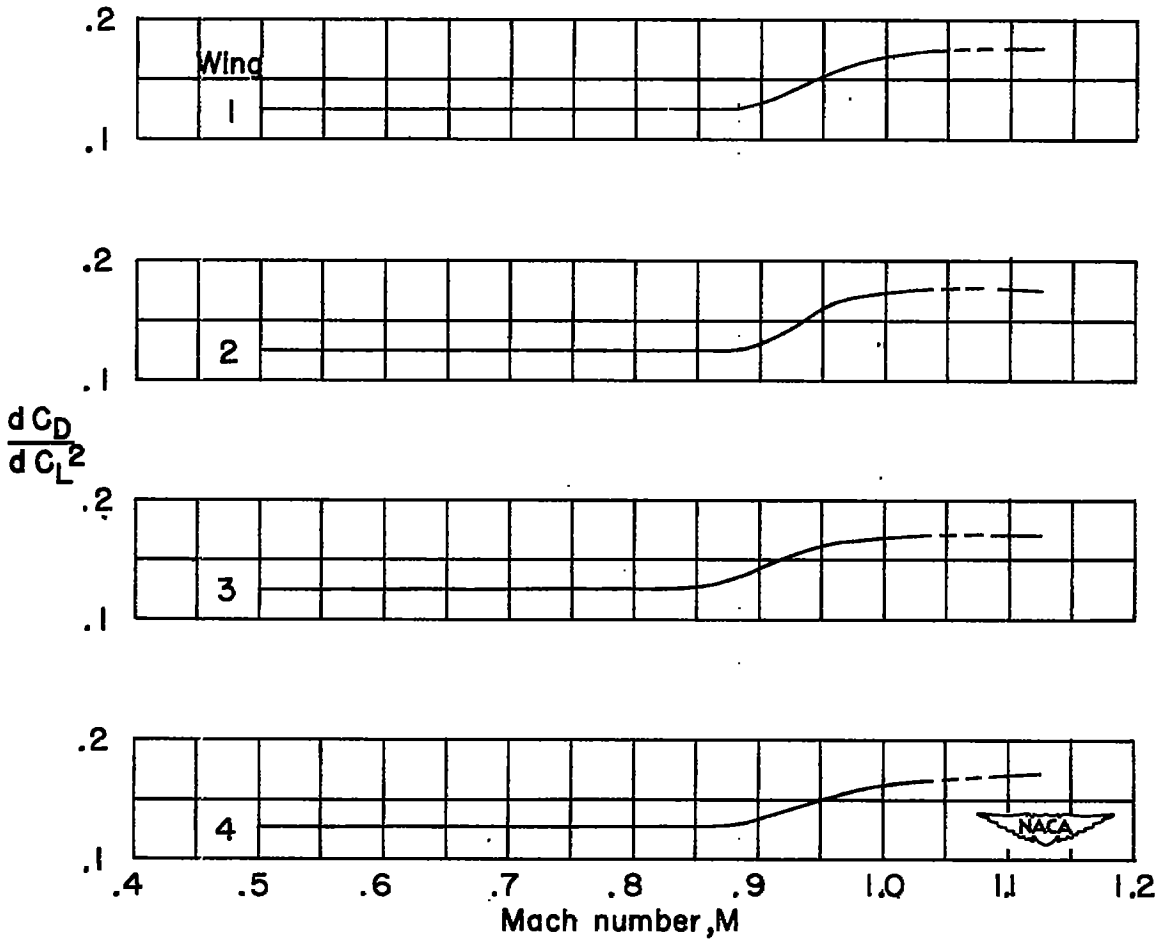

Figure 12.- Effect of thickness ratio and thickened root sections on the variation of drag due to lift with Mach number for the wing-body configuration. $C_L = 0.3$.

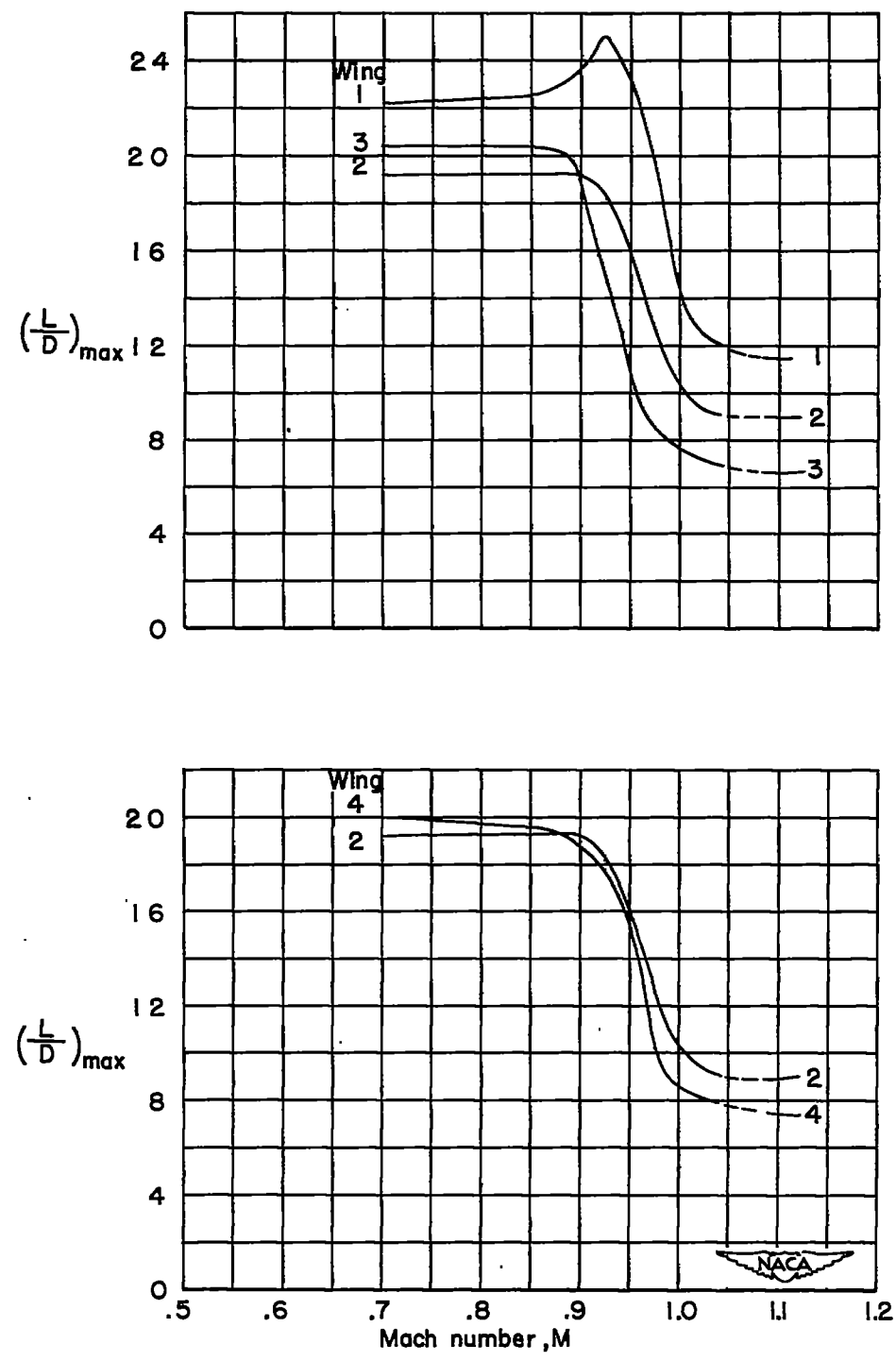

Figure 13.- Effect of thickness ratio and thickened root sections on the variation of maximum lift-drag ratio with Mach number for the wing-body configuration.

[redacted]

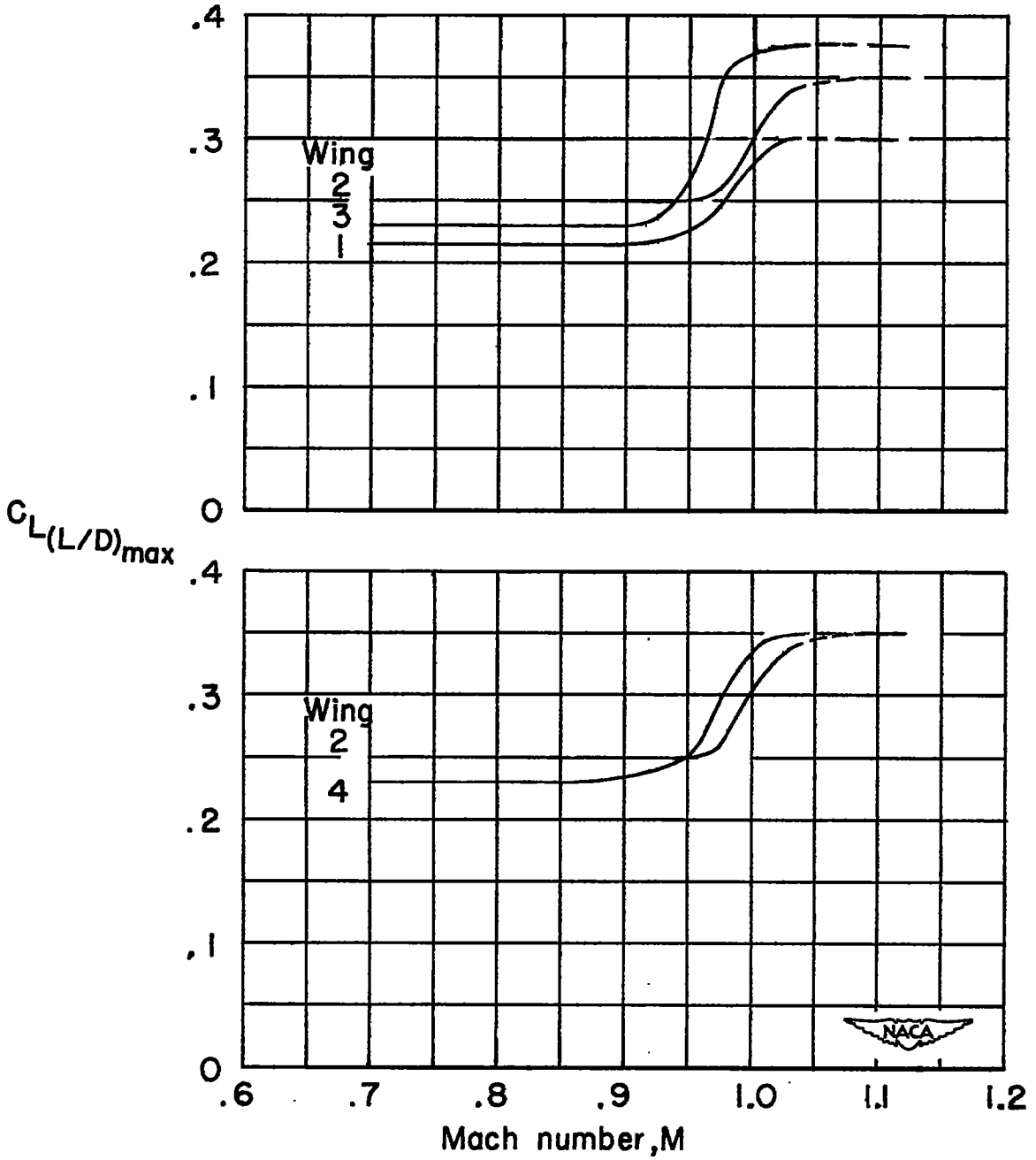

Figure 14.- Effect of thickness ratio and thickened root sections on the variation of lift coefficient for maximum lift-drag ratio with Mach number for the wing-body configuration.

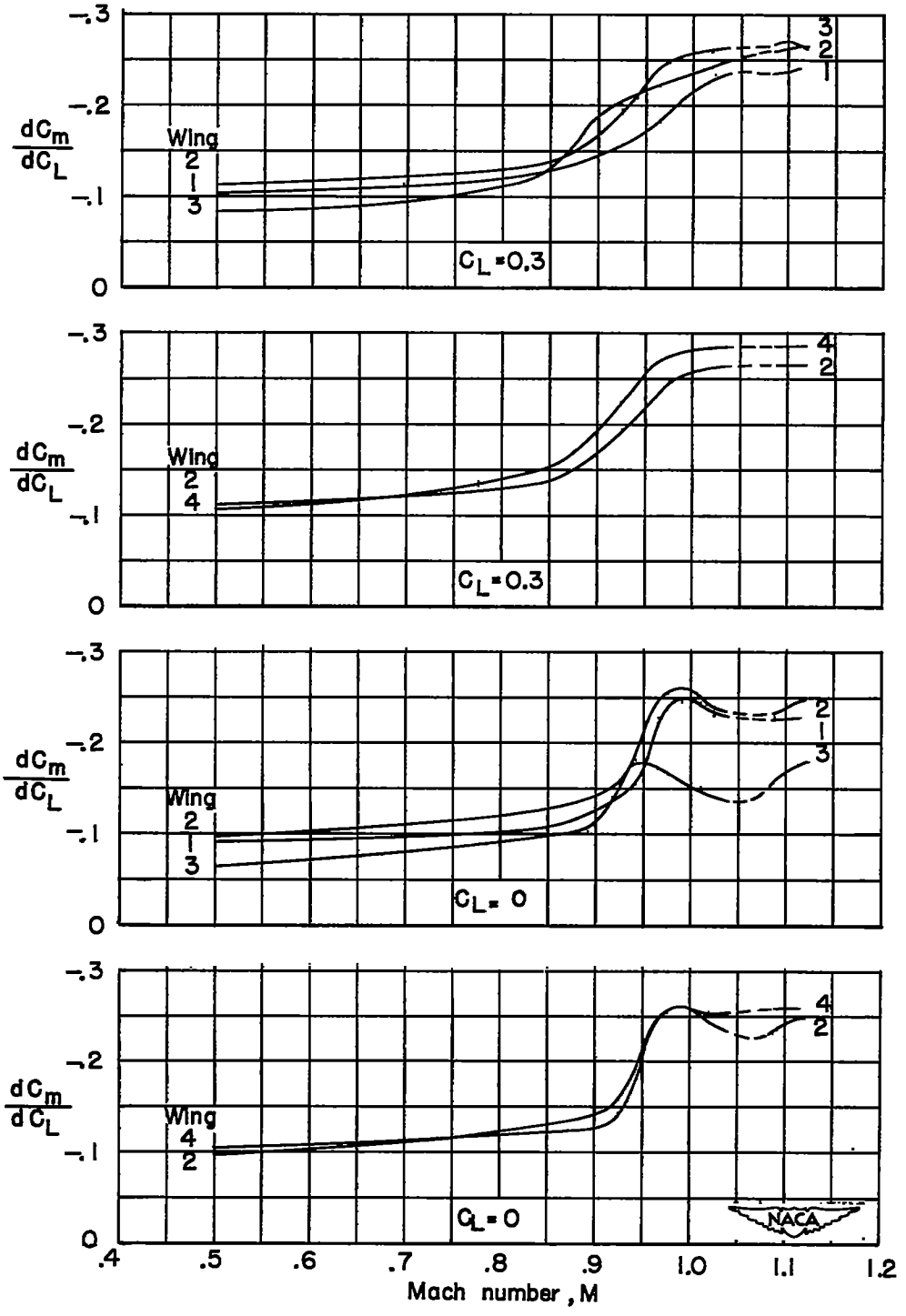

Figure 15.- Effect of thickness ratio and thickened root sections on the variation of the static-longitudinal-stability parameter with Mach number for the wing-body configuration.

[redacted]

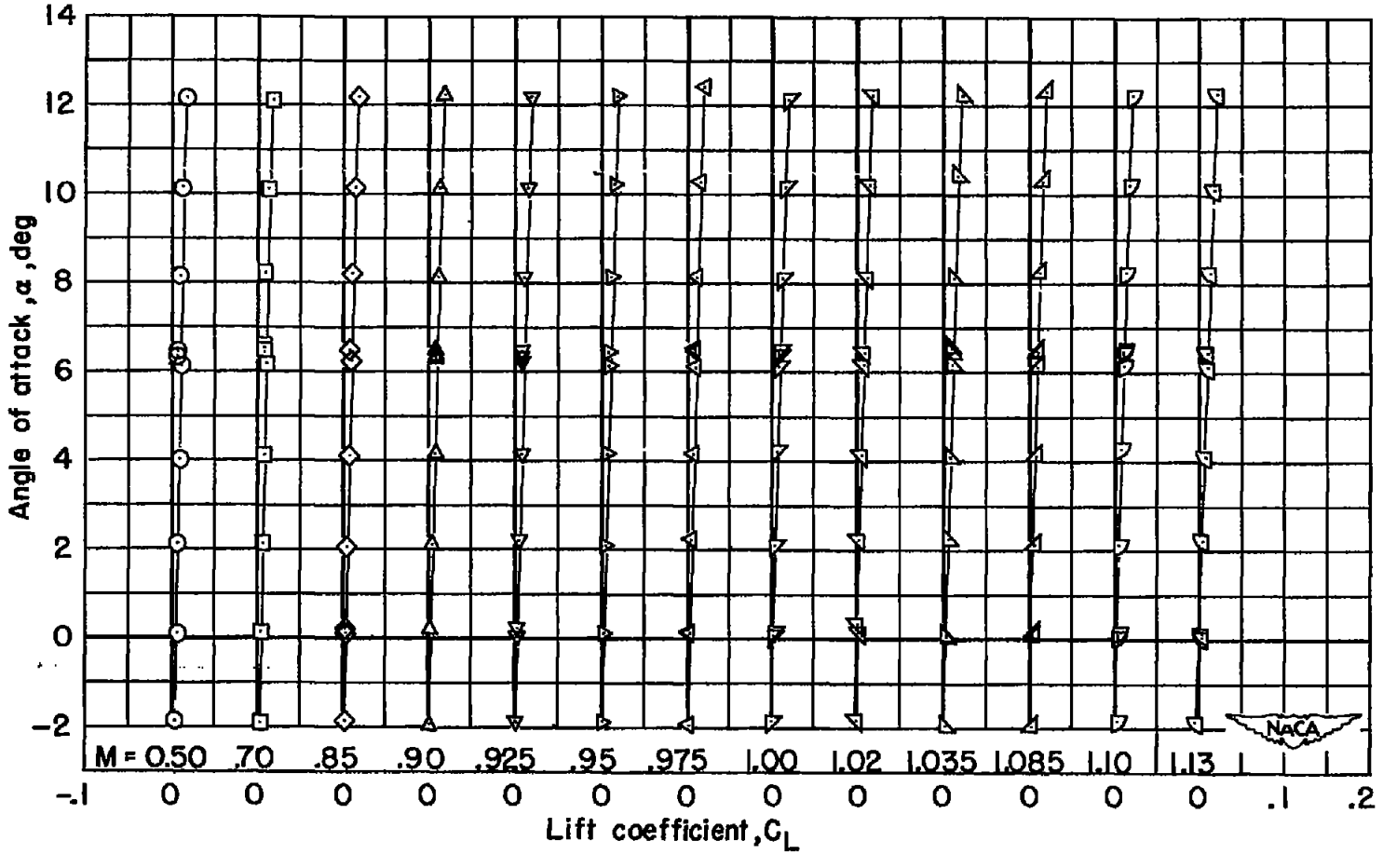

(a) Lift coefficient.

Figure 16.- Variation with angle of attack of the aerodynamic characteristics of the body.

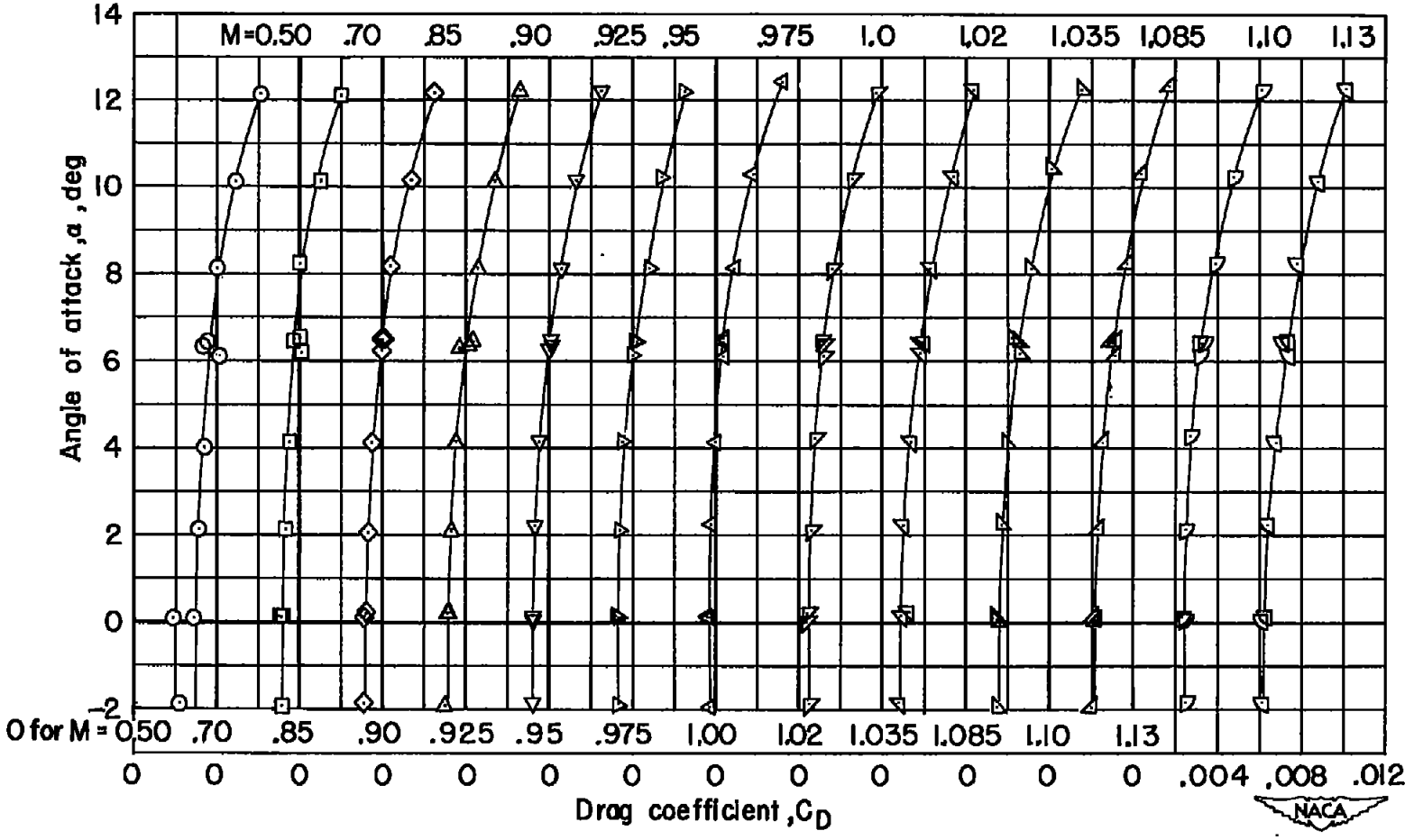

(b) Drag coefficient.

Figure 16.- Continued.

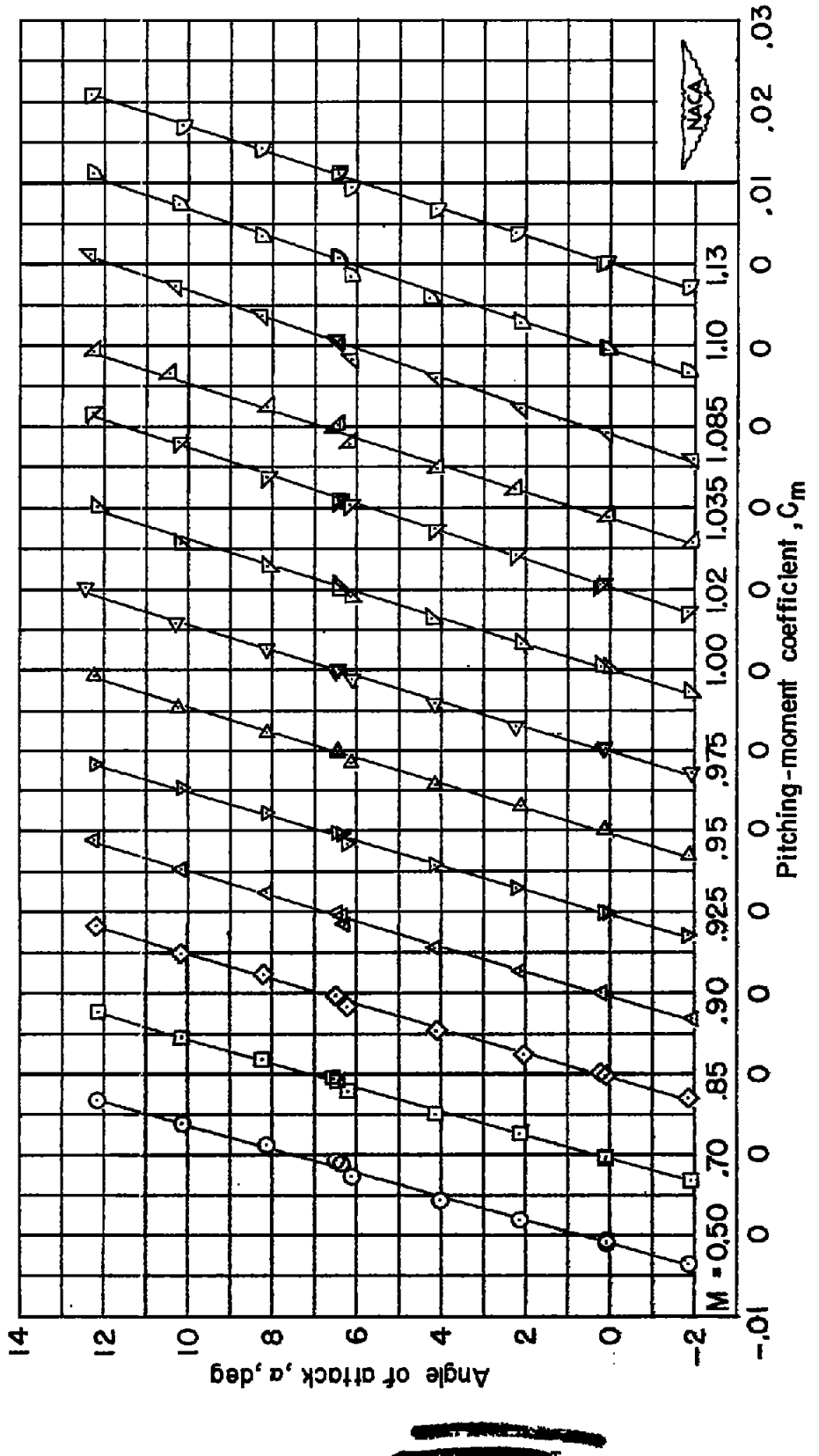

(c) Pitching-moment coefficient.

Figure 16.- Concluded.